HTS Transmission Lines for Ship-Board Radar Applications

Navy Contract N00014-96-C-2001

Final Report

May 7, 1997

Submitted by:

Salvador H. Talisa, Program Manager
Northrop Grumman Corporatiion
Science and Technology Center
1350 Beulah Road
Pittsburgh, PA 15235-5080

Prepared for:

Naval Research Laboratory
4555 Overlook Avenue, S.W.
Washington, DC 23075-5000

Northrop Grumman STC
1350 Beulah Road
Pittsburgh, Pennsylvania 15235-5080

HTS Transmission Lines for Ship-Board Radar Applications

Navy Contract N00014-96-C-2001

Final Report

May 7, 1997

Submitted by:

Salvador H. Talisa, Program Manager
Northrop Grumman Corporatiion
Science and Technology Center
1350 Beulah Road
Pittsburgh, PA 15235-5080

Prepared for:

Naval Research Laboratory
4555 Overlook Avenue, S.W.
Washington, DC 23075-5000

Northrop Grumman STC
1350 Beulah Road
Pittsburgh, Pennsylvania 15235-5080

HIGH TEMPERATURE TRANSMISSION LINES FOR SHIP-BOARD APPLICATIONS

Final Report

1. Introduction

This is the final report of a study to determine the feasibility of using high temperature superconductors (HTS) for providing low-loss transmission lines to remotely feed a phased array radar antenna, mounted above the deck of a ship, from the transmit/receive modules which would be located below deck. The study parameters were provided by NRL and are given in Table 1. A previous similar study involving low-temperature superconducting (LTS) transmission lines was completed a year ago. That final report is included here as Appendix 2 in order to facilitate the overall evaluation of this idea.

The present study has been approached from the point of view of establishing the superconductor material properties which, if available in suitable form, would allow the fabrication of transmission lines with the required level of loss and power dissipation performance. The starting point was materials produced to date on dielectric and metallic tape and as thick films on wire and other substrates. Measured surface resistances were available directly from some of the manufacturers or were found in the literature. This is in contrast to the previous study for which the availability of good quality niobium to fabricate coaxial lines was a given and the manufacture of the lines, and their cryogenic cooling to 6 K, was considered an engineering (and financial) problem and not a technological one. Many practical aspects related to the fabrication of the transmission-line structures proposed here as suitable candidates were not considered in detail because, although important, they are out of the scope of this initial study.

Two candidate transmission-line structures were chosen to conduct the study. A wide microstrip line enclosed in a cylindrical metallic tube was chosen as a candidate because it might be fabricated with the planar-type HTS conductors which currently are being produced at several laboratories by deposition of thick HTS films on metallic or dielectric substrates with, or without, buffer layers. A coaxial transmission line configuration was also considered even though, at present, there has been no report of a process which produces films of sufficiently low loss on the required curved surfaces. Techniques are currently being developed by which the center and outer conductors could be fabricated by deposition of an HTS film on the outside of a metallic wire (e.g. Ag) and the inside of a tube, respectively, from a slurry. Significant improvements in the resulting film properties will have to be achieved, however, in order to meet the specifications of

our application. Alternatively, the center conductor might be fabricated as a wire by sintering of bulk HTS although this process is currently yielding conductors with microwave properties not much better than copper at 77K.

For both the microstrip and the coaxial cable we have projected the attenuation, power loss, and refrigeration requirement as a function of the dielectric loss tangent and the rf surface resistance of the HTS films.

TABLE 1 - Study Parameters

Frequency of Operation	1300 MHz
Bandwidth	200 MHz
Maximum Antenna/Transmitter Separation	75 ft.(22.5 m)
Maximum Average Input Power/Line	50 W
Maximum Peak Input Power/Line	500 W
Maximum Allowed Attenuation/Line	1 dB
Number of Lines (Array Elements)	2000

2. Wide Microstrip Transmission Line

Conductor Configuration and Fabrication

The microstrip line being considered is shown in Figure 1. It consists of two HTS tape conductors sandwiched around a dielectric characterized by its relative dielectric constant ε_r and loss factor tan δ. Typical dimensions for the dielectric would be $w \cong 1$cm and $h \cong 0.1$cm. The requirements for the dielectric are that it be manufacturable in long lengths (up to 25 m) with these cross-sectional dimensions, and that it have reasonable values of ε_r and tan δ. Those requirements will be discussed here in more detail later on, but it should be mentioned that some candidates are quartz, alumina, and air.

As shown in Figure 1, the wide microstrip line would be encased in a normal-metal tube which would isolate the lines from each other to prevent undesirable cross-talk. The design of this enclosure has not been undertaken here. Its diameter will have to be chosen so as to minimize its effect on the line insertion loss. The role and effectiveness of this enclosure are equivalent to the normal-metal microwave package in microstrip HTS cellular-telephone base-station filters at 940 MHz. They have loss requirements exceeding those of the problem treated here and are made with excellent quality and negligible impact of the package on insertion loss.

The HTS-tape conductors would be fabricated by deposition of a film of HTS material on a suitable substrate using thin- or thick-film techniques. Thin-film techniques (e.g. sputtering and

pulsed-laser deposition) generally result in high-quality epitaxial HTS films with thicknesses below 1 μm. Thick-film techniques such as CVD, electrophoresis and screen-printing result in films of lower microwave quality; they have thicknesses generally greater than 2 μm. Obviously, the highest quality films attainable would be desirable. The ultimate would be epitaxial films on single-crystal substrates but this would be very difficult, if not impossible, to achieve in the required lengths. The most promising technique for achieving films of usable quality, on substrates which may be fabricated to meet the requirements of this application, is that referred to as the ion-beam-assisted deposition (IBAD) process which produces textured buffer layers on non-metallic substrates. Recent microwave measurements reported[1] from Los Alamos National Laboratories for 0.4 μm thick YBCO grown on IBAD-textured YSZ buffer layers on polycrystalline alumina are very encouraging. They find that the microwave surface resistance (R_s) of the YBCO is about 3 mΩ at 10 GHz and 76K. Although this is almost an order of magnitude greater than that typically found for high-quality epitaxial thin films on $LaAlO_3$, it is nearly an order of magnitude smaller than for copper. Because R_s in superconductors scales as f^2, at 1 GHz the thick YBCO films will have $R_s \cong 30\ \mu\ \Omega$, which is two orders of magnitude smaller than for copper.

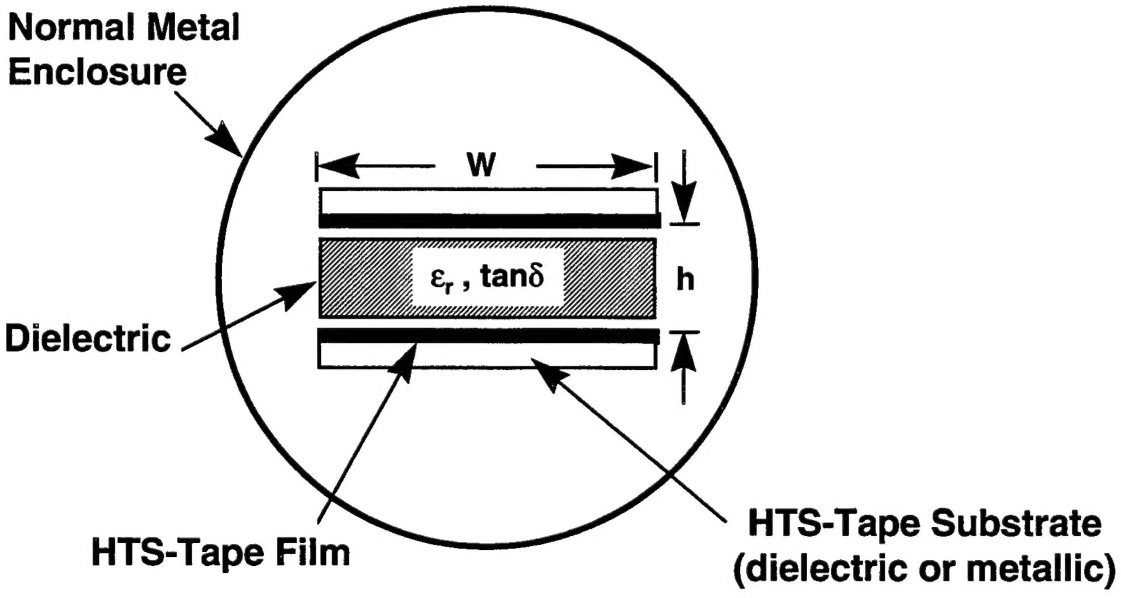

Figure 1 - Schematic representation of the cross section of the microstrip transmission line concept. Most of the electromagnetic energy concentrates between the superconducting plates so that negligible loss is incurred in the normal-metal enclosure.

The IBAD process has been used recently by Freyhardt, et al.[2] in Germany to deposit textured buffer layers of YSZ on large area (20 cm × 20 cm) metallic and non-metallic substrates and on curved or cylindrical surfaces (dia. ≤ 1.5 cm). Although the microwave properties of the

YBCO films grown by pulsed laser deposition on the textured YSZ have not been reported, the critical-current density (j_c) values measured indicate that the films are highly ordered and may have microwave properties similar to those reported by LANL.

At Oak Ridge National Laboratories[3] another process called rolling-assisted-biaxially-textured-substrates (RABiTS) is being used to provide metallic substrates which, when buffered with CeO_2 or YSZ, can be used to grow YBCO films with critical current densities $j_c > 10^5$ A/cm^2 in zero magnetic field. Examples of these substrates are YSZ/CeO_2/Pd/Ni and CeO_2/Ag/Pd/Ni. We considered this process because it has produced films with relatively high critical current densities indicating reasonable film quality. However, calculations (see Appendix 1) indicate that the microwave losses incurred in the metallic substrates currently being considered will be so large as to preclude their use. The RABiTS process would be much more appealing for our application if suitable metallic substrates can be found that have lower rf losses (i.e. lower R_s) than those currently used, as will be shown later.

An important consideration in determining whether a particular process will yield useful HTS films is the rf power dependence of the surface resistance. For epitaxial thin films produced by sputtering, laser ablation, or other means, R_s is on the order of 5 μΩ at 1 GHz and relatively independent of the rf magnetic field for $H_{rf} < H_{C1} \cong 100$ Oe or more, H_{C1} being the lower critical magnetic field. According to the demands of the present application, for 500 W of input power to a transmission line the rf magnetic field at the HTS film will be $H_{rf} \cong 10$ Oe, well below H_{C1} for epitaxial films. Although we are not aware of any published data on the power dependence of R_s in the films produced by the IBAD or RABiTS processes, it is well known that losses at grain boundaries and other imperfections are responsible for increasing R_s with H_{rf}. For example, in thick films produced by screen printing, or those textured films obtained by appropriate heat treatment of deposited precursors from a slurry, it is found[4,5] that R_s increases rapidly with H_{rf} from a few hundred μΩ in a zero field to more than 1 mΩ for $H_{rf} > 1$ Oe, near 1 GHz. Thus, the power dependence of the IBAD and RABiTS films must be determined before a judgment can be made regarding their use for this application.

Although it is not clear what effort must be put forth in time and money to develop a capability to manufacture microstrip HTS conductors in sufficiently long lengths for our goals, it is clear that more than one basic process has been defined to produce the desired geometry, at least in short lengths.

Electrical Characteristics

The characteristic impedance Z_L and the attenuation α_c due to losses in the conductors for a wide microstrip line with $w/h \geq 3.3$ can be calculated using Wheeler's formulas and the

method of incremental inductance.[6] Approximate expressions for these quantities in the limit w/h >> 1 are:

$$Z_L = \frac{120\pi}{\sqrt{\varepsilon_r}} \frac{h}{w} \tag{1}$$

where ε_r is the relative dielectric constant, h is the separation between the parallel superconductors, and w is the width of the line, respectively (see Figure 1). The attenuation due to conductor losses is given by

$$\alpha_c\left(\frac{dB}{m}\right) \cong 8.68 \times 10^3 \frac{R_s}{wZ_L}, \tag{2}$$

with R_s and Z_L in ohms and w in mm.

Figure 2 shows the characteristic impedance Z_L calculated as a function of w/h, the ratio of strip width to dielectric thickness, for three values of ε_r which represent the three dielectric materials mentioned previously. Of note here is that for w/h = 10 we find that Z_L = 10 Ω. This is not too low a value to be easily matched to 50 Ω at each end. From here on we take as our model for calculation purposes a line with w = 1 cm and h = 0.1 cm so that w/h = 10.

There are two other microwave loss contributions which must be considered. One is the loss incurred in the dielectric between the conductors and the other is the loss in the substrates upon which the HTS films are deposited. If the substrates are non-metallic dielectrics, the loss will be negligible because the fields outside the conductors are quite small. However, if the substrates are metallic the losses can be quite significant because of the relatively high microwave surface resistance expected for the materials typically used such as Ni or its alloys. We calculate the loss

in a metallic substrate as a ratio to that in the superconductors and the ratio of dielectric losses to superconductor losses in the Appendix 1.

The loss in the microstrip dielectric may be approximated by[6]

$$\alpha_d\left(\frac{dB}{m}\right) = 8.686 \frac{\pi\sqrt{\varepsilon_r} f}{c_o} \tan\delta, \tag{3}$$

where f is in GHz and c_o is the speed of light in vacuum (30 cm/ns).

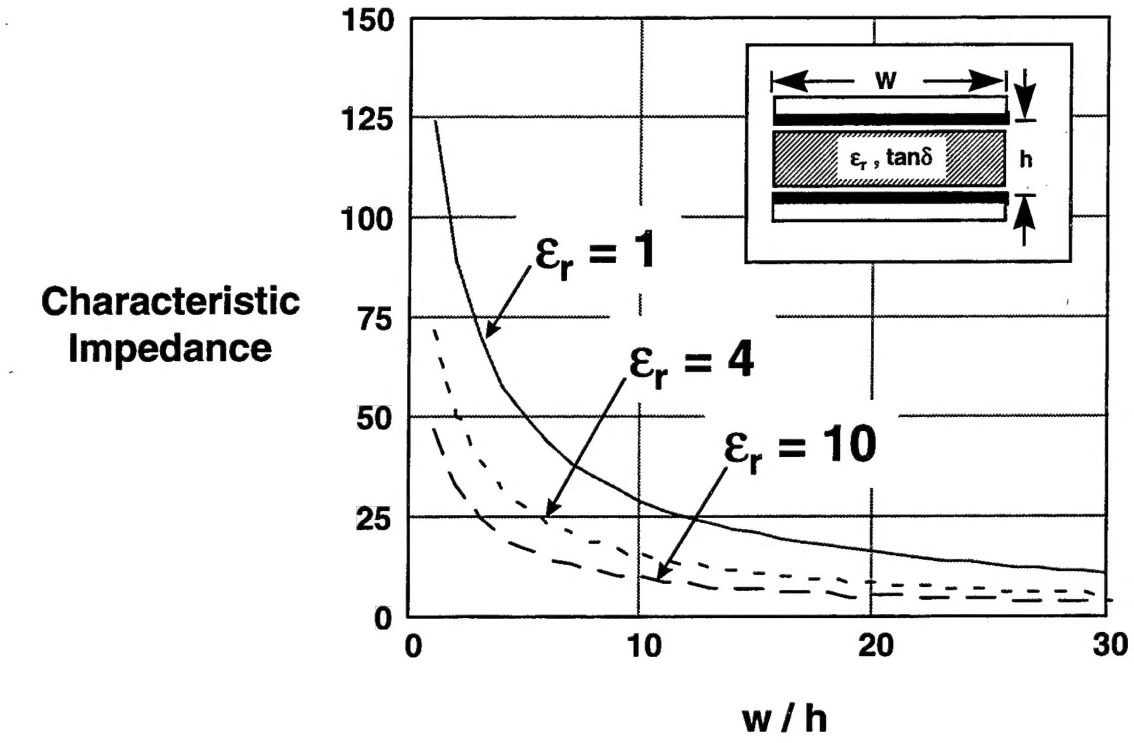

Figure 2 - Characteristic impedance of the parallel-plate microstrip line as a function of the width-to-dielectric spacing ratio for air ($\varepsilon_r = 1$), quartz ($\varepsilon_r = 4$) and alumina ($\varepsilon_r = 10$). The calculations presented later on in this study were performed assuming w/h = 10.

For the case in which the HTS films are on dielectric substrates, we calculate the total loss for a 22.5-m-long line as

$$\alpha_T(dB) = 22.5\left(\alpha_d + \alpha_c\right) \tag{4}$$

This is plotted in Figure 3 as a function of the HTS surface resistance R_s for six sets of dielectric parameters. The two straight lines for tan $\delta = 0$ indicate the loss in the superconductor in the absence of dielectric loss. Note the very encouraging result that the total attenuation is less than 1 dB for $R_s \leq 0.6$ mΩ except for the highest curve which corresponds to a dielectric constant of 10 and a loss tangent of 10^{-4}. Even for that case, the 1 dB value is achieved for $R_s \leq 0.25$ mΩ.

The power dissipated in N lines, each of which is 22.5 m long, for an average input power of P_i watts, is given by:

$$P = NP_i\left(1 - 10^{-0.1\alpha_T}\right). \tag{5}$$

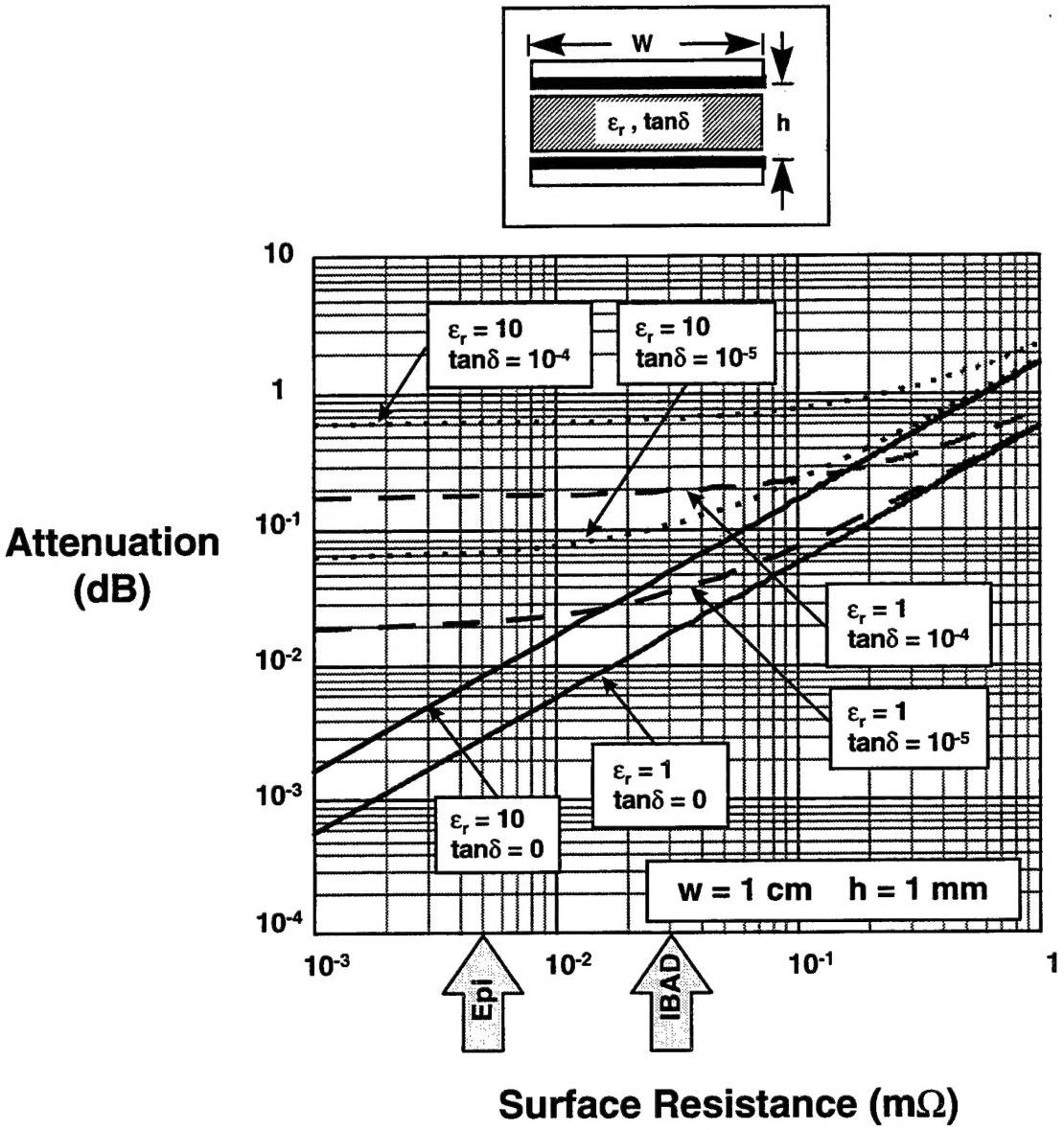

Figure 3 - Calculation of parallel-plate microstrip attenuation vs. HTS surface resistance for various parameters indicated on the plot. Also indicated, for calibration, are the surface resistances of epitaxial HTS films and that reported for IBAD material, respectively. Copper has a R_s = 4 mΩ at 77K and 1 GHz and falls outside of the graph range.

The results for N = 2000 and P_i = 50 W are plotted in Figure 4 as a function of R_s, again for six sets of dielectric parameters. Note that for tan $\delta = 10^{-4}$ the power dissipated is predominantly in the dielectric for $R_s < 0.1$ mΩ. And even in the best case of tan $\delta = 10^{-5}$ and $\varepsilon_r = 1$, the loss is dominated by the dielectric for $R_s < 3 \times 10^{-2}$ mΩ. As noted earlier, HTS conductors are being made in short lengths in this configuration with R_s about equal to this value at 1 GHz. Thus, an improvement in the quality of the HTS film with a corresponding reduction in R_s will not lead to reduced losses in this microstrip unless a dielectric with tan$\delta \leq 10^{-5}$ and $\varepsilon_r \cong 1$ is used. Obviously, use of an air dielectric is the answer but that may be very difficult to manufacture. Further studies and trade-offs are required.

It can been seen from Figure 4 that the total power dissipated, even in the worst case, is on the order of 20 kW while it could be as low as a few kW for $\varepsilon_r \leq 4$ and tan $\delta \cong 10^{-5}$. The refrigeration requirement to handle this dissipation is discussed below following the section describing the results for a coaxial configuration.

Figure 5 presents the resulting total power dissipation when the loss in the metallic substrates, if used for the HTS films, is included in the calculations used to generate Figure 4. A value of 30 mΩ, characteristic of non-magnetic alloys, has been taken for the substrate surface resistance at 1 GHz and 77K. (See Appendix 1). If Ni were used as the substrate, its R_s would be even higher than about 80 mΩ since it is ferromagnetic. The overall loss is completely dominated by the metallic substrate losses, leading to a clear indication that ferromagnetic or metallic alloy substrates will negate the advantage of using HTS to provide low transmission line losses unless the effective R_s of the substrate can be lowered by the use of suitable buffer layers.

3. Coaxial Transmission Line

Conductor Configuration and Fabrication

We will consider coaxial lines of standard dimensions, up to 0.325 in. (0.826 cm) OD, and characteristic impedance of 50 Ω. The ratio of inner conductor diameter to that of the outer conductor will depend, of course, on the relative dielectric constant. From an HTS fabrication standpoint,[5] we consider center conductors in the range of 1-3 mm OD and outer conductors with 2-8 mm ID. It is unlikely that the IBAD process or any process involving physical vapor deposition of HTS films could be used to obtain films with usable properties on curved surfaces with such small radii or on the inside of a tube. However, thick film processes are being developed which will allow a silver wire or silver-plated stainless-steel wire to be coated for the center conductor; similarly a silver plating on the ID of a stainless-steel tube will provide the outer conductor. Thick films of this type have shown[4] R_s values of 370 μΩ at 1.3 GHz on 1 cm diameter rods in coaxial resonators and it is not unlikely that this process could be extended to smaller diameters. Illinois Superconductor, Corp.[5] has produced textured YBCO thick films on plated stainless steel and on

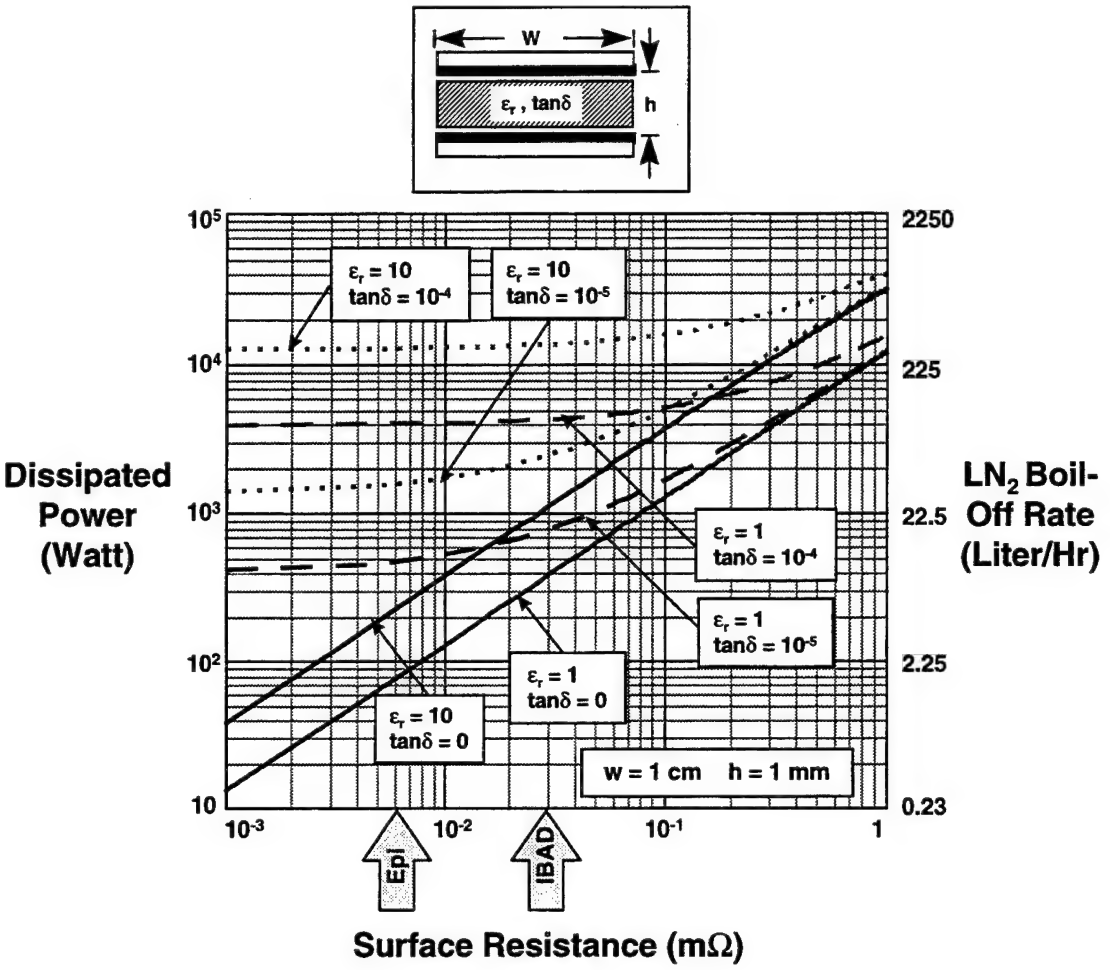

Figure 4 - Calculation of power dissipated in 2000 parallel-plate microstrip lines vs. HTS surface resistance for various parameters indicated on the plot. The power dissipated was calculated from the attenuation given in Figure 3. The corresponding liquid nitrogen boil-off rate is given on the right-hand axis. Also indicated, for calibration, are the surface resistances of epitaxial HTS films and that reported for IBAD material, respectively. Copper has a R_s = 4 mΩ at 77K and 1 GHz and falls outside of the graph range.

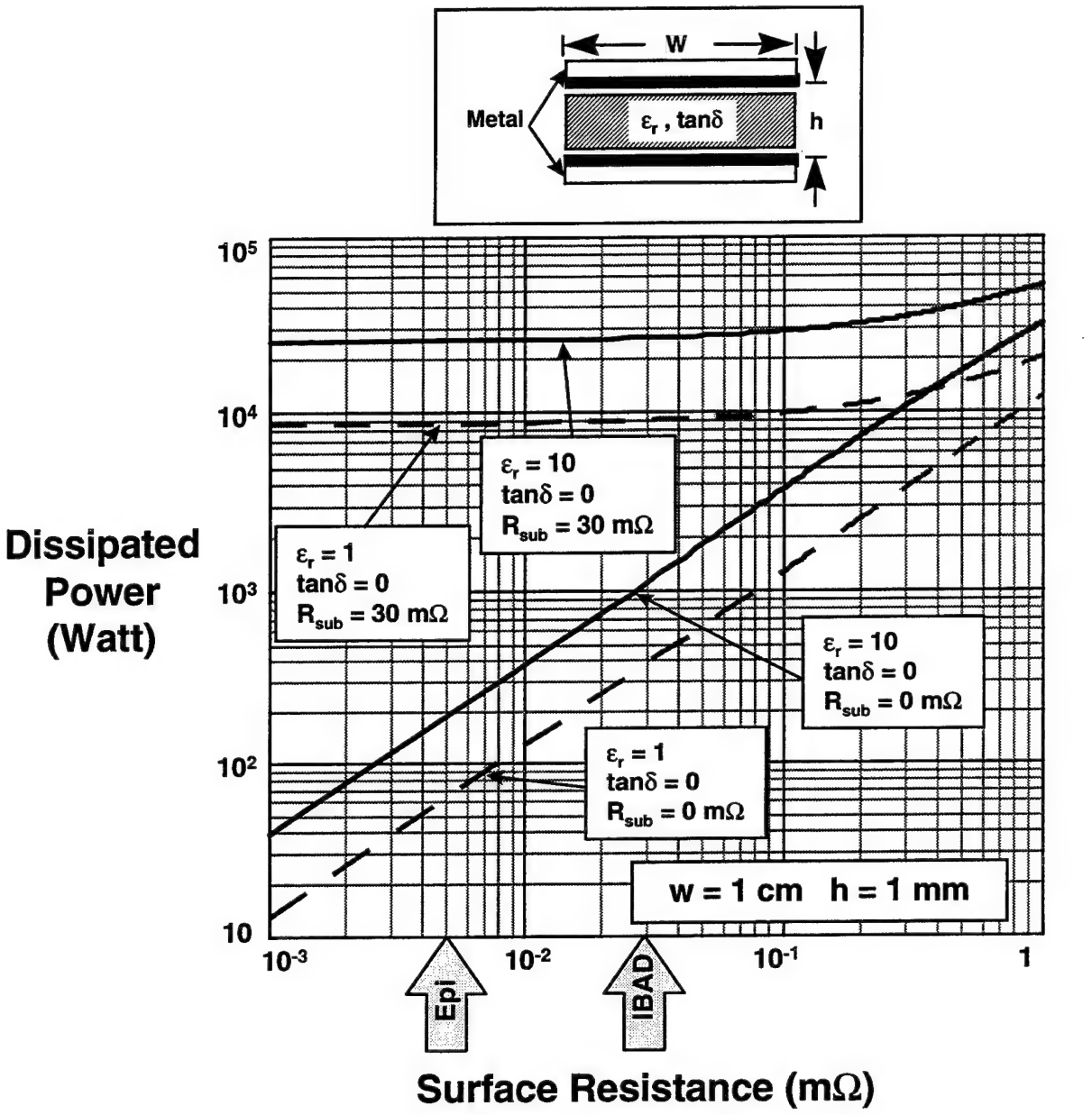

Figure 5 - Calculation of power dissipated in 2000 parallel-plate microstrip lines vs. HTS surface resistance for the case of superconductor deposited on Ni tape (surface resistance R_{sub} = 30 mΩ). The power dissipated is quite high, even for lossless dielectric (tan δ = 0). Compare with the plot in Figure 4. Also indicated, for calibration, are the surface resistances of epitaxial HTS films and that reported for IBAD material, respectively. Copper has a R_s = 4 mΩ at 77K and 1 GHz and falls outside of the graph range.

zirconia with measured $R_s < 0.5$ mΩ at 940 MHz and 77K and projects that the process could be extended to long lengths of wire and tube. However, as discussed earlier, the power dependence of R_s in these films currently precludes their use at the power levels (50-500 W) expected in this application. Improvements in the processing of the films would have to be developed to significantly increase their power handling capability.

The dielectric to be used for fabrication of the coaxial lines should be chosen to minimize the effect of dielectric losses on the refrigeration requirements but must also allow cost effective manufacturability. This will be discussed further following the modeling to determine the attenuation and loss contributions of the dielectric relative to the conductors.

Electrical Characteristics

The calculation of Z_L and attenuation coefficient α for a coaxial transmission line is straightforward. Z_L is given by:

$$Z_L = \frac{\eta}{2\pi} \ell n\left(\frac{b}{a}\right) \tag{6}$$

where a and b are the inner and outer conductor radii, respectively, and η is the intrinsic impedance of the dielectric given by:

$$\eta = \sqrt{\frac{\mu}{\varepsilon_o \varepsilon_r}} \tag{7}$$

with μ the permeability in the dielectric medium and ε_o the vacuum dielectric constant. Taking $Z_L = 50\ \Omega$ and assuming $\varepsilon_r = 2.0$ (the value for PTFE (Teflon) at 77K) we find, for example, the OD of the inner conductor for standard 0.325 in. coax (ID of outer conductor = 0.72 cm) to be 0.22 cm.

The attenuation due to the dielectric is given by equation (3), and the attenuation due to the conductors is

$$\alpha_c = 8.686 \frac{R_s}{4\pi Z_L}\left(\frac{1}{a} + \frac{1}{b}\right). \tag{8}$$

Figure 6 plots the total attenuation $\alpha_T = \alpha_c + \alpha_d$ for 22.5 m of 0.325-in. coaxial cable as a function of R_s for three values of tan δ. Again, the straight line is for tan $\delta = 0$ and represents the conductor losses in the absence of dielectric losses. We have assumed in the foregoing that the surface resistance is the same for both inner and outer conductors.

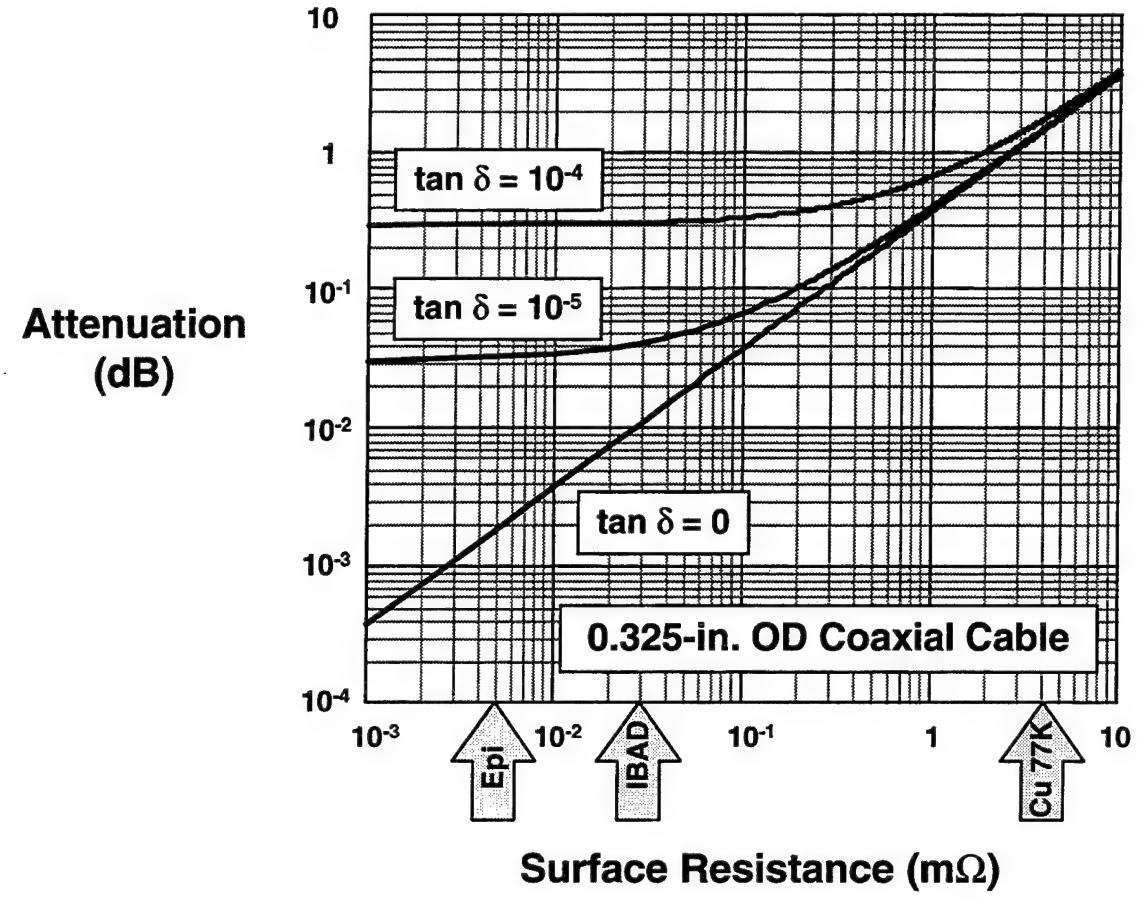

Figure 6 - Calculation of 0.325-in. coaxial cable attenuation vs. HTS surface resistance for three values of dielectric loss factor. Also indicated, for calibration, are the surface resistances of epitaxial HTS films, that reported for IBAD material, and copper at 77K, respectively.

Figure 6 shows that even for a relatively high loss tangent of 10^{-4} the overall attenuation is less than 1 dB for $R_s \leq 1$ mΩ. For tan $\delta = 10^{-5}$, not an unreasonable value for microporous PTFE (Teflon) at 77K (see Appendix 2), the dielectric losses are negligible for $R_s > 0.1$ mΩ.

The power dissipated in 2000 of these coaxial lines, each 22.5-m long, is plotted in Figure 7 as a function of R_s, again for three values of loss tangent. The results are quite similar to those for the microstrip line in the absence of substrate losses. A dissipation as high as 20 kW is suffered for tan $\delta = 10^{-4}$ and $R_s = 1$ mΩ, but falls rapidly as these parameters are reduced.

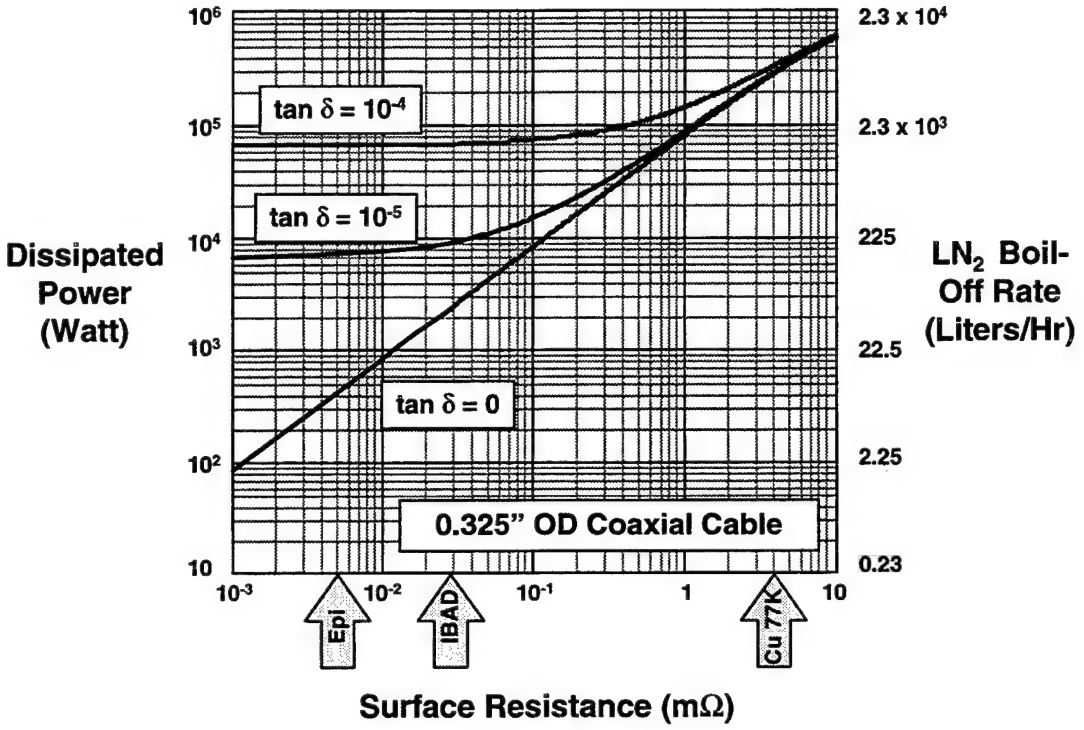

Figure 7 - Calculation of power dissipated in 2000 0.325-in. coaxial lines vs. HTS surface resistance for three values of dielectric loss factor. The power dissipated was calculated from the attenuation given in Figure 6. The corresponding liquid nitrogen boil-off rate is given on the right-hand axis. Also indicated, for calibration, are the surface resistances of epitaxial HTS films, that reported for IBAD material, and copper at 77K, respectively.

4. Cryogenic Considerations

Refrigeration Requirements

In the previous study (Appendix 2) we considered the possibility of using LTS materials in this application. There it was found that the dielectric losses would dominate in a coaxial cable made with the superconductor Nb. However, the major consideration in determining feasibility was the size and cost of the refrigerator required to maintain the temperature of the Nb below its critical temperature, T_c = 9.2K. For the HTS transmission lines being considered here, the refrigeration requirements are much less severe. Consider cooling the entire bundle of lines by pool-boiling liquid nitrogen. That is, the 2000 0.325 in. (0.826 cm) coaxial lines would be arrayed in a circular cross section and placed inside a metal duct approximately 40 cm in diameter. If microstrip is used for the HTS lines, the OD of each line would be about twice as large, yielding a duct of about 75 cm in diameter. The resulting cross-sectional area of the interstices through

which liquid nitrogen could flow to provide cooling is about 294 cm^2 for the coax and 1100 cm^2 for the microstrip. The flow rate to provide the required cooling is calculated from the properties of LN_2 at 77K. The latent heat of vaporization is 160 kJ/l and the number of liters of liquid vaporized per kilowatt-hour of heat input is 22.5 l/kW-hr.

Referring again to Figures 4 and 7, we note the scale on the right side indicates the rate of LN_2 boil-off to maintain the lines at 77K for the power dissipated as a function of R_s. To put this in perspective, we compare the calculated requirements to the capacity of a liquifier supplied to the Navy, for shipboard operation, by Gas Equipment Engineering Corp. The machine provides about 110 l of liquid per hr from room-temperature gas. Using the cold gas produced by the boil-off instead would approximately double the liquifying rate to provide about 10 kW of cooling. This machine, manufactured to military specifications, costs about $1.8 million.[7]

The liquid nitrogen would be forced through the interstices of the close-packed lines at a few atm of pressure. In addition to the 1.76 atm due to the weight of the column of liquid, there would be a pressure drop due to the liquid flow. It is straightforward to calculate the pressure drop at the required flow rates. Through the 294 cm^2 of cross-sectional area for the coaxial case, for example, the result is that at a flow rate of 2250 l/hr (about 10 gals/min) the flow is laminar and the pressure drop over 22.5 m is negligible at less than 1 psi. The pressure drop will be proportionately less for the larger area available for the microstrip case. This provides enough cooling that even for 10 kW of dissipation only 10% of the liquid would be vaporized as it passed through the system. The 77K gas would then be circulated back to the refrigerator for reliquifying.

Transitions from 77K to Room Temperature

At each end of the HTS transmission lines, be they microstrip or coaxial, a transition must be made to the room-temperature transmitter or antenna which, in the case of the parallel-plate line proposed here, would include an impedance transformer to 50 Ω. For the LTS case previously considered, capacitive coupling to copper coax would have to be used because the conductive heat leak to the helium-cooled lines at 6K would be quite high. The transition from 77K to 300K does not present nearly as severe a thermal problem.

Considering a coaxial line made of copper-coated stainless steel for the outer and inner conductors and PTFE dielectric, we ignore for the moment the heat generated within the conductor and that due to radiation and calculate the heat conducted from the room temperature end to the cold bath.

The inner and outer conductor dimensions for a standard 0.325" (0.826 cm) coax are:

d_o = ID of outer conductor = 0.724 cm

d_i = OD of inner conductor = 0.284 cm

The thermal conductivities for copper, PTFE (teflon), and stainless steel are approximately independent of temperature for 77 < T < 300K and in are given by (see Figures 4-6 in Appendix 2)

$$\kappa_{Cu} = 5, \qquad \kappa_{SS} = 0.1, \qquad \kappa_{Diel} = 10^{-3},$$

in W/cm-K. The skin depth of copper at room temperature and 1 GHz is about 2 μm. So we take the thickness of the Cu plating on the ID of the outer conductor and the OD of the inner conductor to be 5 μm and we find the total heat leak to be 6.0 W-cm. Thus, for 2000 lines, each 20 cm long, we have a heat leak into the cryogen of 600 W. The attenuation and power dissipated per unit length for 2000 of these copper coaxial lines with 50 W input is easily calculated. The attenuation α_T (dB/cm) may be calculated in the same manner as for the HTS coaxial lines above. Assuming a room temperature value of $R_{s,cu} = 8.24$ mΩ at 1 GHz and tan $\delta = 2 \times 10^{-5}$ for microporous PTFE, we find $\alpha_T = 1.16 \times 10^{-3}$ dB/cm. The power dissipation for 2000 lines as a function of their length is plotted in Figure 8 along with the heat leak and their sum which is the total heat load to be handled by the refrigeration due to the transitions at one end. Note that the total heat load is a minimum of about 1 kW for about 20 cm of length for the copper coaxial line. For the two ends there will be 2 kW, which must be added to the loss in the HTS transmission lines when determining the refrigeration requirements. The attenuation for 40 cm of copper line (20 cm at each end) is a negligible 0.05 dB. The impedance transformer to 50 Ω needed for the parallel-plate transmission line would not be expected to significantly change the estimated attenuation and power dissipation figures.

System Configuration

A schematic drawing of the baseline configuration of the transmission line system is shown in Figure 9 along with representative dimensions. Whether the HTS lines are coaxial or microstrip, the copper coaxial line transitions to room temperature will be the same. But in the case that the HTS is microstrip, a transition from microstrip to coaxial will be required, besides the impedance transformer mentioned above. We have a good deal of expertise in the fabrication of the required transitions through our work on previous Navy programs (HTSSE I and HTSSE II for example) and do not foresee this as a problem.

The 2000 HTS transmission lines would be enclosed in a vacuum-jacketed duct of less than 0.5 m in diameter for the coaxial line case and less than 1 m for the microstrip. The basic notion of forcing the cryogen through the interstices appears to be the most efficient method of cooling.

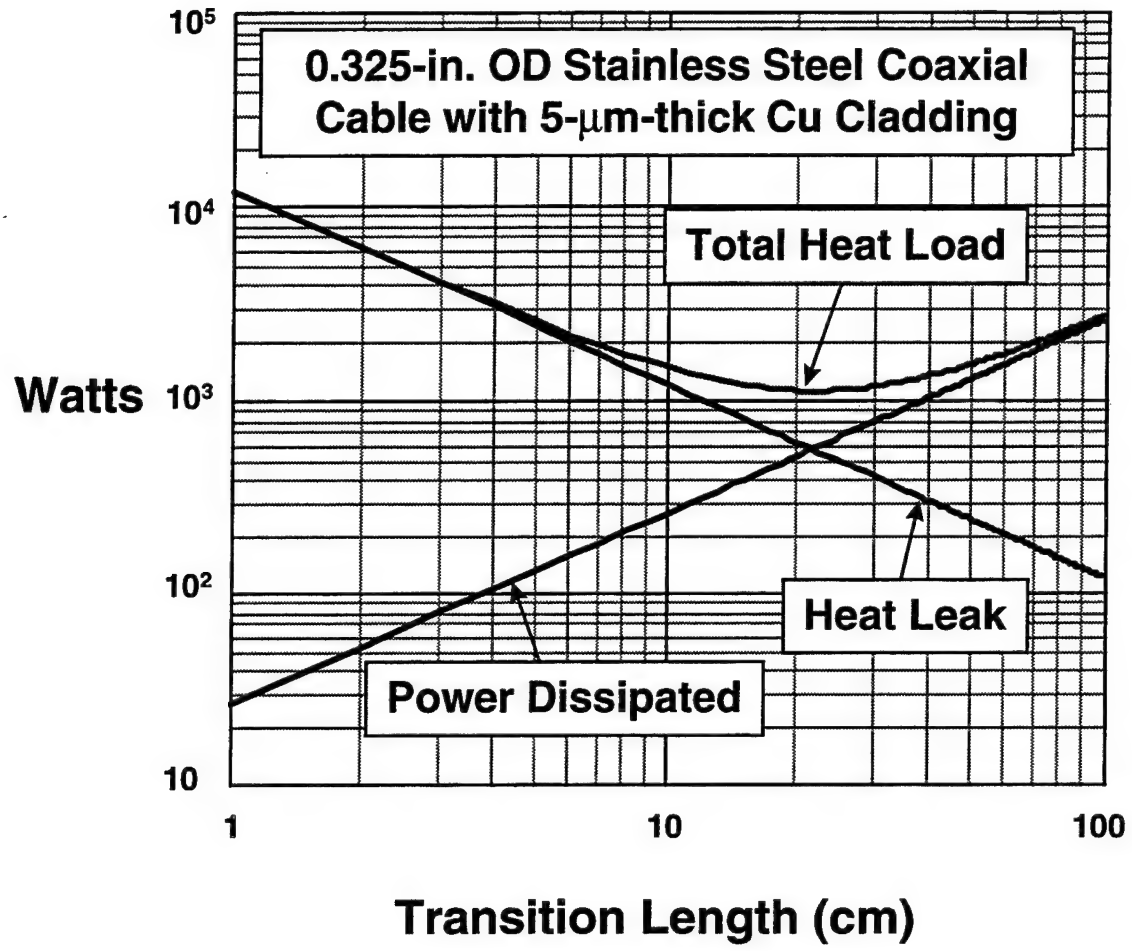

Figure 8 - Calculation of heat load due to 2000 transition coaxial lines at one end of the cryogenic transmission line system as a function of transition line length. These transition lines were assumed to be 0.325-in. OD stainless steel coaxial cable with 5-μm-thick copper cladding on the OD of the inner conductor and the ID of the outer conductor. The total heat load is made up of the power dissipated in the 2000 transition lines plus the conductive heat leak from room temperature to 77K. The total refrigeration requirements due to transition lines is double the calculated amount in order to account for transitions at the antenna and transmitter ends.

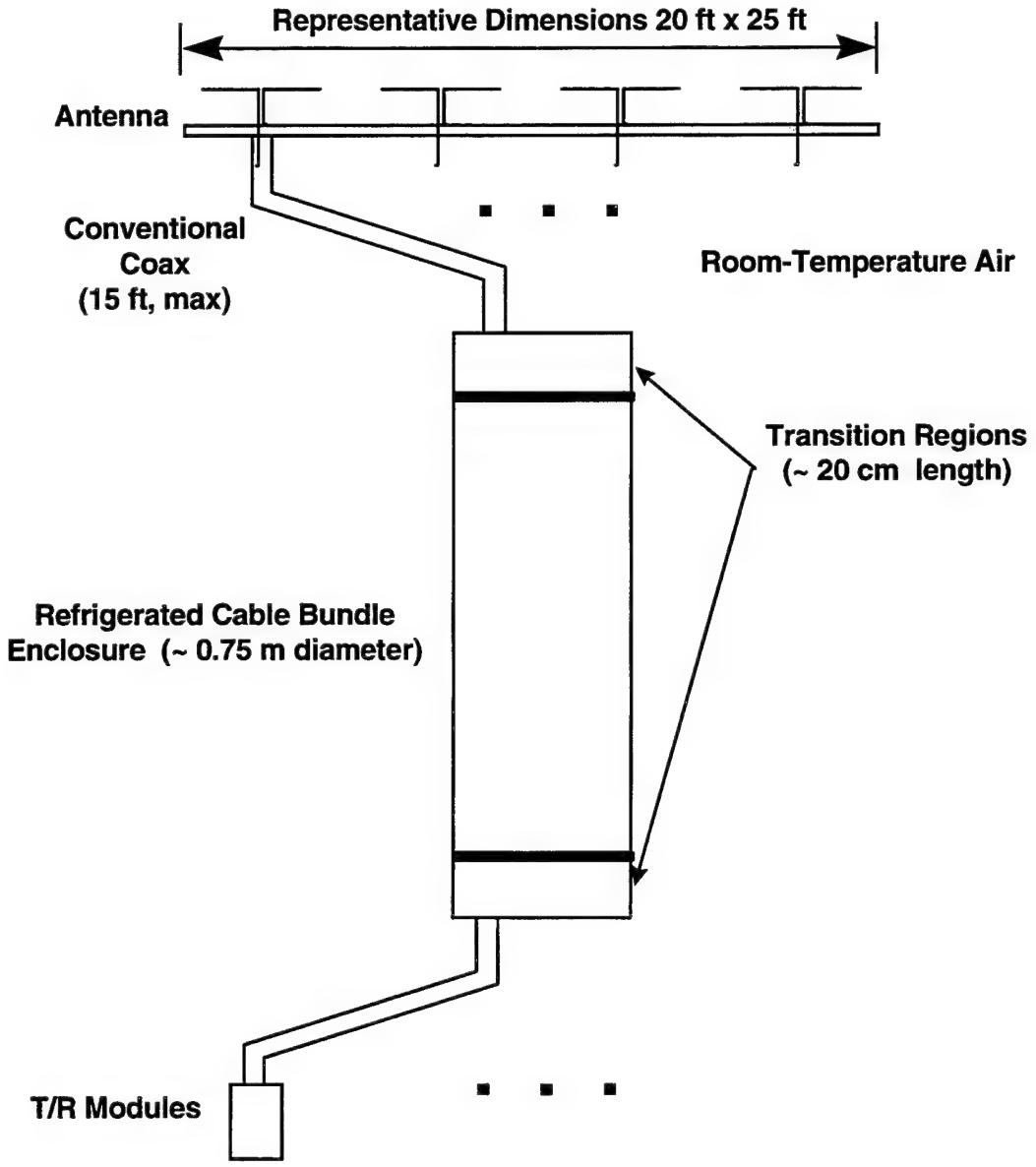

Figure 9 - Schematic representation of the cryogenic transmission line system concept.

5. Conclusions and Recommendations

In the previous study (Appendix 2), which considered a coaxial line fabricated with low temperature superconductor (LTS) Nb ($R_s \leq 1$ μΩ at 1 GHz), we found that the conductor losses were insignificant compared to the losses in the dielectric and in the normal-metal coaxial cable which must be used to make the transition from low temperature (≅ 6K) to room temperature. A refrigeration requirement of about 200 W at T = 6K, using single-phase liquid helium, was projected. The result is that the size, cost, and availability of the refrigeration system are the dominant considerations in using LTS for this application. At the other extreme is the notion of using an all-copper coaxial cable system at T = 77K for the 22.5 m span required to feed the antenna. In that case R_s(1 GHz) ≅ 4 mΩ and the conductor losses would dominate for dielectric loss tangents even as high as 10^{-4}. The resulting attenuation of > 3 dB would be excessive, as would be the > 300 kW of cooling required (see Figures 6 and 7). The intermediate case is the one being considered in this study, where high-temperature superconductors (HTS) would be used for the conductors either in a coaxial line or a parallel-plate line. In this case, for reasonable values of R_s and tan δ, the dielectric and conductor losses are typically the same order of magnitude so that neither dominates. A modest value of surface resistance, $R_s \leq 1$ mΩ, for the HTS conductors would yield ≤ 1 dB of attenuation with a corresponding cooling requirement of ≤ 10 kW for tan $\delta \leq 10^{-5}$.

The required tan $\delta \leq 10^{-5}$ at T = 77K can be met by one of several dielectric candidates which can also be fabricated in long lengths, namely; quartz, alumina, or PTFE. The required $R_s \leq 1$ mΩ is easily achieved in short, flat samples by the IBAD process currently being used to obtain YBCO thick films on alumina substrates buffered with YSZ. Reported[1] R_s(10 GHz) ≅ 3 mΩ predicts R_s(1 GHz) ≅ 30 μΩ. It remains to be determined whether the power dependence of R_s for these films will allow operation at 500 W and whether the same quality films can be made in sufficiently long lengths. Although no R_s measurements have been reported for the films deposited on substrates being produced by the RABiTS process[3], the film quality and resulting dc critical current densities achieved in short lengths suggest that it too may yield HTS films with $R_s \leq 1$ mΩ at 1 GHz. However, our rough calculations indicate that the metallic substrates currently being used for this process would be unsuitable due to their excessive rf losses. Experimental verification of this conclusion along with more accurate calculations are required.

At present we are not aware of any process which will produce HTS films of suitable quality on curved surfaces for fabricating coaxial lines. For example[4], thick films of YBCO deposited by slurry techniques on zirconia rods 1 cm in diameter have shown measured R_s ≅ 0.370 mΩ at very low power levels. However, the R_s increases rapidly with power and would not be much better than copper for our application. The IBAD process has been used[2] to deposit

films on curved surfaces with good dc properties but no rf measurements have been reported and it is difficult to envision how it could be applied to a coaxial line structure. However, the possibility of using this process in connection with the parallel-plate line should be pursued.

The refrigeration requirement of ≤ 10 kW is modest and may be provided by a liquid nitrogen consumption of 225 l/hr. A refrigerator currently in shipboard use by the Navy is capable of providing this.

We conclude by noting

- that presently the most promising configuration for the transmission lines is the enclosed parallel-plate line.
- at the present time, the IBAD process is the most promising for producing the HTS conductors although the RABiTS process should not be dismissed.
- that the refrigeration requirements, projected from short-sample properties of the HTS conductors, are not a dominant consideration as is the case for the LTS lines.

We suggest that an experimental verification program be carried out. The first phase of such a program should concentrate on establishing the viability of existing material by performing rf measurements on small samples. A later phase should include the fabrication of representative lengths (a few meters) of the conductors and their formation into transmission lines; followed by a determination of their microwave transmission properties at relevant power levels and projections of performance in lengths of more than 20 m. The microwave performance verification might also include signal phase measurements.

References

1. A. T. Findikoglu, et al Appl. Phys. Lett. **69**, 1626 (1996).
2. H. C. Freyhardt, et al., submitted for publication in IEEE Trans. Appl. Superconductivity
3. A. Goyal, et al Appl. Phys. Lett. **69**, 1795 (1996).
4. P. A. Smith, et al submitted for publication in IEEE Trans. Appl. Superconductivity.
5. H. Muller, Illinois Superconductor Corp., private communication.
6. R. K. Hoffmann, "Handbook of Microwave Integrated Circuits," Artech House 1987.
7. Gas Equipment Engineering Corp., Milford CT., Contact: Bob Newell, T: 203-874-6786. A unit similar to the one we require is now being prepared for delivery to the U. S. Navy for the USS Carl Vincent, via solicitation # N00406-97-R5033 from Fleet and Industrial Supply Center, Puget Sound. This solicitation contains the latest navy specification references. This unit provides approximately 200 lb./hr of either LN_2 or LO_2. The unit meets stringent Navy

requirements such as operation at 30° angles, pitch, roll, and shock (depth charges). The unit has distillation columns and air-bearing turboexpanders, but does not have its own main air compressor--the air is supplied by other compressors on the vessel. Power consumption is negligible compared to the compressor power needed, which is about 350 horsepower. Cost of this mil-spec unit is about $1.8 million. The unit, without compressor, is about 12' x 7' x 7' and weighs about 20,000 lb.

APPENDIX 1

LOSS IN METALLIC SUBSTRATE

The process of making good polycrystalline conductors from the high-temperature superconductor YBCO involves depositing a crystal-oriented layer of material on a substrate, either a metallic substrate with a dielectric buffer layer or a dielectric substrate with or without an additional buffer layer. The RABiTS process developed at ORNL is very promising for producing long lengths of HTS strip conductors. It achieves highly-textured metallic substrates of Ni or Ni alloys upon which highly oriented polycrystalline buffer layers and subsequently YBCO can be grown. Here we estimate the losses incurred in the metallic substrates when the HTS conductors are used in a microstrip transmission-line geometry as discussed in the text.

The geometry which is being considered for making a guided microwave transmission line using YBCO is that of two parallel strips. But one problem with a parallel strip transmission line is that the magnetic field outside the space between the strips is non-vanishing. Thus, the presence of a normal metal layer on the backside of the strip can lead to an appreciable loss in the normal metal which adds to the loss in the superconductor. The main purpose of the present calculation is to examine the loss in the normal metal. Of course, the metallic substrate loss could be eliminated by simply using a dielectric (e.g. alumina) substrate, but a flexible metallic substrate might provide greater reliability against shock and shipboard accidents.

Estimate Of Magnetic Field Outside The Parallel Strips

For a long transmission line with a long wavelength (relative to the cross-sectional dimensions) the magnetic field outside the strips can be obtained approximately by using the Biot-Savart expression where the current density $\vec{j}$ is taken

to be along the z axis (length of the strip) but assumed to depend only on x, y, and time.* Thus, for a single strip in Gaussian units

$$\vec{H}_j = curl\frac{1}{c}\int \vec{j}(x',y')\frac{dx'\,dy'\,dz'}{\left[(x-x')^2+(y-y')^2+(z-z')^2\right]^{1/2}} \qquad (1)$$

where the integration is over the volume of the superconductor in the strip. $\vec{H}_j$ is the magnetic field produced by the supercurrent, in Oe. In practical units of Oe, A/cm^2, and cm

$$\vec{H}_j = 0.1\,curl\int \vec{j}(x',y')\frac{dx'\,dy'\,dz'}{\left[(x-x')^2+(y-y')^2+(z-z')\right]^{1/2}}. \qquad (2)$$

An integration over z between $\pm\infty$ gives, after some manipulation,

$$\vec{H}_j = -0.1\,curl\int \vec{j}(x',y')\ln\left[(x-x')^2+(y-y')^2\right]dx'\,dy' \qquad (3)$$

and performing the curl leads to

$$H_{jx} = -0.1\int j(x',y')\frac{2(y-y')dx'\,dy'}{\left[(x-x')^2+(y-y')^2\right]}$$

$$\vec{H}_{jy} = +0.1\int j(x',y')\frac{2(x-x')\,dx'\,dy'}{\left[(x-x')^2+(y-y')^2\right]}. \qquad (4)$$

If x is along the width of the strip and y along the thickness, j(x',y') must be such that the y component of $\vec{H}_j$ vanishes within and just outside the strip because very little flux normal to the strip can go through the superconductor. The symmetry of the current which causes this cancellation is given by j(-x',y') = - j(x',y'), as opposed to the transport

---

* In the dielectric H = $H_0 \cos\left(\omega t - \sqrt{\varepsilon}\omega z / c\right)$ and the current density along the strip has a similar dependence on z. The wavelength $c / f\sqrt{\varepsilon}$ for $\sqrt{\varepsilon}$ ~ 1 and f = 1 GHz is about 30 cm. Thus it is a fair approximation to neglect the z dependence.

part which has the symmetry j(-x',y') = j(x',y'). However, it is expected that the transport part is bigger than the part which cancels the y component and, to good approximation, the x component of field can be calculated using only the transport part j_t. Thus,

$$\vec{H}_j \approx -0.1\,\hat{x}\int j_t(x',y')\frac{2(y-y')\,dx'\,dy'}{\left[(x-x')^2+(y-y)^2\right]}. \tag{5}$$

As a simplifying assumption any x dependence of j_t will be neglected. Further, since the superconductor layer is assumed to be very thin, and the field outside the superconductor is of principal interest, y-y' will be replaced by y in the integrand of (5), and the equation becomes

$$\vec{H}_j \approx -0.1\,\hat{x}\int j_t(y')dy'\int \frac{2y}{\left[(x-x')^2+y^2\right]}dx'. \tag{6}$$

The integral of j_t over y' gives I/W where I is the transport current and W the width of the strip. Then performing the integral over x' between W/2 and -W/2 gives

$$H_{jx} \approx -0.2\frac{I}{W}\frac{y}{|y|}\left[\tan^{-1}\frac{1}{|y|}\left(\frac{W}{2}-x\right)+\tan^{-1}\frac{1}{|y|}\left(\frac{W}{2}+x\right)\right] \tag{7}$$

Averaged over x, this expression becomes

$$\left\langle H_{jx}\right\rangle = -0.2\frac{I}{W}\frac{y}{|y|}\left[2\tan^{-1}\frac{W}{|y|}-\frac{|y|}{W}\ln\left(1+\frac{W^2}{y^2}\right)\right] \tag{8}$$

and for large W^2/y^2 compared with unity

$$\left\langle H_{jx}\right\rangle \approx -0.2\frac{I}{W}\frac{y}{|y|}\left[\pi-\frac{2|y|}{W}-\frac{2|y|}{W}\ln\frac{W}{|y|}\right] \tag{9}$$

which is taken to be the field of interest. Consider now the field of two parallel strips. Inside the strips, y for the upper strip is negative and I is positive while for the lower strip y is positive and I is negative. Thus $Iy/|y|$ is the same for both strips and with neglect

of the small term in y and use of the fact that I/W is the surface current density $J_{sc.}$, in the superconductor

$$\langle H_{jx} \rangle_{in} \approx 0.4\pi \frac{I}{W} = 0.4\pi J_{sc.}. \tag{10}$$

Equation (10) is simply an integrated Maxwell equation. Just outside the upper strip, y is positive for both strips and ly/|y| has a different sign for the two strips. In (9) the term in π cancels and for the upper strip $y \approx 0$ while for the lower strip $y \approx h$. Thus

$$\langle H_{jx} \rangle_{out} \approx -0.4 J_{sc.} \frac{h}{W}\left(1+\ln\frac{W}{h}\right). \tag{11}$$

This field, which will now simply be labeled H, represents the "applied field" acting on the substrate.

Loss Ratio

Surface current density J must flow along the z axis of each surface of the metallic substrate (with opposite signs on the two surfaces) to produce a magnetic field which cancels the "applied field" (11) inside the substrate. J is given by the integral Maxwell equation $H = 0.4\,\pi J$ (in Oe and A/cm) i.e.

$$J = \frac{1}{\pi} J_{sc.} \frac{h}{W}\left(1+\ln\frac{W}{h}\right). \tag{12}$$

Using the expression

$$\textit{Time Average Power Loss Per Unit Area} = R_s \langle J^2 \rangle_{time}, \tag{13}$$

where R_s is the surface resistance, it follows from (12) that the loss ratio for substrate and superconductor per unit surface area is

$$\textit{Loss Per Unit Area Ratio} = \frac{1}{\pi^2}\left(\frac{h}{W}\right)^2\left(1+\ln\frac{W}{h}\right)^2 \frac{(R_s)_{sub.}}{(R_s)_{sc.}}. \tag{14}$$

However, in the superconductor loss occurs only on one side (to good approximation) while in the substrate it occurs on both sides of a layer. Thus, the substrate has double the area and the total loss ratio of substrate to superconductor is

$$Loss\ Ratio = \frac{2}{\pi^2}\left(\frac{h}{W}\right)^2\left(1+\ln\frac{W}{h}\right)^2\frac{(R_s)_{sub.}}{(R_s)_{sc.}}. \qquad (15)$$

For a normal metal $R_s = 1/\sigma\delta$ where σ is conductivity and δ the skin depth. Assuming a non-ferromagnetic material with $\sigma \sim 0.5 \times 10^5$ mho/cm at 77 K gives $(R_s)_{sub} \sim 30$ mΩ for 1 GHz. For the best polycrystalline HTS material $(R_s)_{sc} \cong 0.02$ mΩ, and for these values

$$Loss\ Ratio = 304\left(\frac{h}{W}\right)^2\left(1+\ln\frac{W}{h}\right)^2. \qquad (16)$$

The loss ratio becomes unity for W/h approximately equal to 97. For smaller values of W/h the loss is dominated by the substrate loss, and since a reasonable W/h is expected to be no more than about 10, it follows that for a good superconductor the total loss is always dominated by the substrate, for a typical metal alloy substrate.

We have used Eq. (15) in the text of this report to show that use of metallic substrates with high R_{sub} values would negate the advantage of using HTS for the microwave conductors.

Conclusions

The conclusions drawn from the preceding analysis are:

1. For a well-textured YBCO on a metallic substrate with a surface resistance typical of a non-ferromagnetic alloy ($R_{sub} \cong 30$ mΩ at 77 K and 1 GHz), nearly all the conductor loss in a microstrip line with w/h = 10 is in the substrate.
2. For the same substrate and under the same conditions as above, for 1 mm $\leq$ h $\leq$ 2 mm, the substrate loss is comparable to the dielectric loss in the microstrip line for $\varepsilon \cong 1$ and $\tan\delta = 10^{-4}$.
3. The RABiTS process would be much more promising for this application if a pure non-ferromagnetic substrate such as silver could be used or if the effective Rs of the substrate could be lowered through the use of suitable buffer layers.

APPENDIX 2

Superconducting Transmission Lines for Ship-Board Radar Applications

Report A003 - Final Report

1. Introduction

A study was conducted to determine the feasibility of using low-temperature superconducting transmission lines in shipboard radar applications. Specifically, the study concentrated on a phased array antenna located atop a mast fed by T/R modules in the ship's hull through a transmission line for each array element. The study was limited to the parameters shown in Table I, which were provided by the Naval Research Laboratory:

Table 1 – Study Parameters

Frequency of Operation	1300 MHz
Bandwidth	200 MHz
Maximum Antenna/Transmitter Separation	75 ft (22.5 m)
Maximum Average Input Power per Line	50 W
Maximum Peak Input Power per Line	500 W
Maximum Allowed Signal Attenuation per Line	1 dB
Number of Lines (Array Elements)	2000

As will be detailed below, one of the main concerns addressed in the study was the refrigerator size needed to keep the transmission line bundle below the superconducting critical temperature. The two main contributors to the required heat lift are:

1. The heat leaks from the transitions between cryogenic and normal ambient temperature regions, and
2. The average heat dissipation in the transmission lines, mostly due to dielectric losses.

Electrical and thermal calculations were performed in order to assess the validity of our assumptions. The best available data were used.

The following issues were to be addressed in the study:

- Superconducting material
- Transmission line configuration
- Power handling capabilities

- Transitions from superconducting to normal transmission lines
- Cooling requirements, type and cost
- Manufacturing
- Experimental demonstration
- Cost

2. Base-Line System Configuration and Assumptions

Several basic assumptions were made at the outset which were later refined as the study evolved. It was desired to direct the study toward standard materials, manufacturing processes and equipment in order to make it economically feasible and minimize new technology development. It was our view that a superconducting transmission line system could be designed and constructed with suitable engineering effort using existing technology, and that the expense would probably be driven by the cryogenic refrigeration system and its maintenance. This is in contrast to a system employing the new high-temperature superconductors (HTS), which would require a considerable amount of research and technology development in order to produce HTS material with the proper dimensional and microwave properties, but which would also be considerably less expensive to cryogenically cool.

The starting assumptions made for this study were:

1. It was established that coaxial cable transmission lines were probably the most suitable from a mechanical as well as electrical point of view. Coaxial cable offers wide bandwidth operation, allows close packing of the transmission line bundle, offers the proper shielding between adjacent lines, and the configuration can be extended to operation at other frequency bands.

2. It was assumed, and later corroborated, that niobium (Nb) is a good candidate superconducting material, readily available in good quality and large quantities, is relatively inexpensive, and is available in tube and wire form. The predicted microwave surface resistance of Nb from published measurements was used in the calculations, but, as will be seen later, the dominant loss mechanism was the dielectric in the coaxial cable.

3. The coaxial transmission line was assumed to be filled with PTFE (Teflon) dielectric in any of its commercially available forms suitable for this application. It was highly desirable to keep the system as simple as possible so that it could be manufactured using existing technology. For example, two coaxial cable manufacturers were contacted who said that Nb cable could be made in the same way as copper or stainless steel standard coaxial, provided suitable Nb tube and wire of the proper dimensions could be supplied.

4. The calculations were kept to standard coaxial cable dimensions to allow as much as possible the use of established manufacturing processes.

The base-line transmission line system envisioned is depicted schematically in Figure 1. The transmission line system would feed a phased array antenna at L-band, at the top end, and would be connected to an array of T/R modules at the bottom. Representative dimensions for the antenna array are 25 ft x 20 ft, with the T/R modules expected to be configured in a similar array pattern. The superconducting transmission line system would then be connected to the antenna and T/R modules through conventional lines. A transition region from the cryogenic to the normal ambient temperature regions would also comprise a length of conventional coaxial cable.

3. Electrical Considerations

The electrical characteristics of superconducting coaxial lines made with Nb have been calculated in order to establish the feasibility of our approach. As explained in the previous section, Nb was chosen as the candidate superconductor for reasons described below, and we limited our considerations to standard cable dimensions and configurations to facilitate a future manufacturing process. Four standard cable dimensions and three Teflon dielectric types were considered. The Teflon configurations are solid, spline (air articulated), and micro-porous; the latter two are products of Precision Tube, Inc. (See Figure 2). Data on conductor and dielectric materials were obtained from the literature and from measurements and published data from Precision Tube, Inc. In some cases it was necessary to estimate parameters from related data. In particular, cryogenic measurements at 1.3K of the dielectric properties of Teflon [1] were used here and assumed to be approximately valid between 4.2 and 6K.

Tables II to IV summarize the results of our calculations. Table II lists the coaxial cable characteristics used in the calculations presented in Table III for Nb at 6K and Table IV for Cu at 300 K. The various sources for these parameters are indicated in the footnotes below Table II.

Table III shows the estimated performance of the superconducting lines at the chosen maximum operating temperature of 6K. Nb, in the purity readily available (99.9%) for coax manufacture has a critical temperature of 9.1K above which it loses its superconducting properties. As can be seen from Table III, the loss in the dielectric limits the performance of the lines. No attempt was made at this point to presume more sophisticated approaches involving new or more expensive dielectric materials or air dielectric lines (even levitation of the center conductor has been proposed [2]). Our intention was to estimate the performance of the lines in their simplest, most accessible configuration, leaving more advanced approaches for a later iteration of the problem.

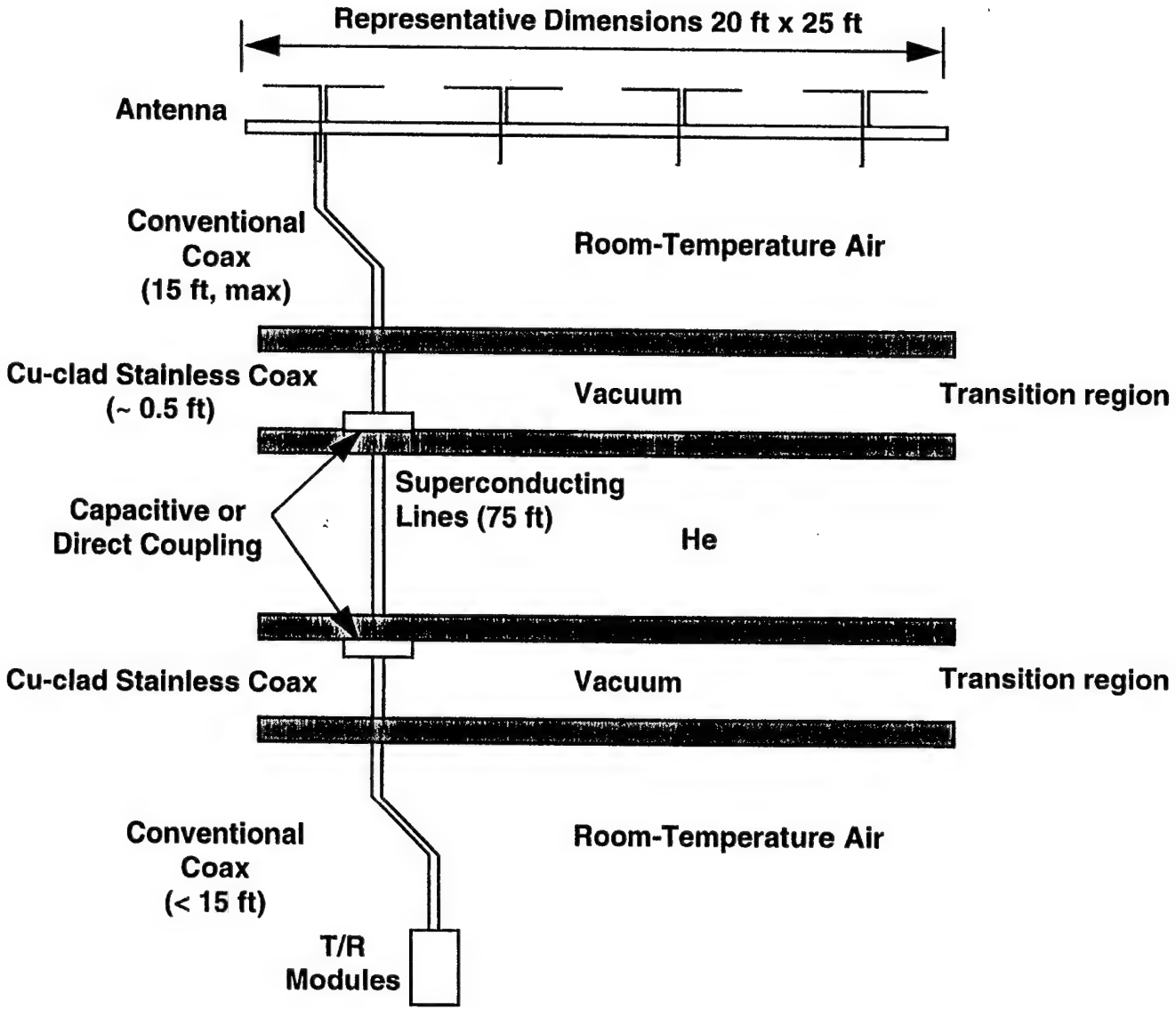
Representative Dimensions 20 ft x 25 ft
Antenna
Conventional
Coax
(15 ft, max)
Room-Temperature Air
Cu-clad Stainless Coax
(~ 0.5 ft)
Vacuum
Transition region
Superconducting
Lines (75 ft)
Capacitive or
Direct Coupling
He
Cu-clad Stainless Coax
Vacuum
Transition region
Conventional
Coax
(< 15 ft)
Room-Temperature Air
T/R
Modules

Figure 1

COAXITUBE™

Air-Articulated Cables

In COAXITUBE air-articulated cables, the inner conductor support within the outer conductor is provided by longitudinal splines of paste-extruded Teflon. This results in a cable with small weight and minimum attenuation, free of periodicity effects (as encountered with spiral or perforated-tape dielectric constructions) and an effective dielectric constant of 1.3. Propagation velocity is about 87%.

Measurements of SA50250 (Page 36) indicate a phase temperature coefficient of virtually zero in the 100°-150°C range, 7PPM/°C from 25° to 100°C and 17PPM/°C from −50° to 0°C. Aluminum conductors, outer and inner, increase the temperature coefficient in the low temperature range to 19.5 PPM/°C and the high temperature range to 12.8 PPM/°C (SH50250-5).

Air-articulated cables do not experience the outer conductor distortion common to solid electric cables, hence temperature stabilization of the dielectric is much less effective and is not necessary except in the most critical applications.

Hermetic sealing of the cable ends or terminations will prevent the cable from "breathing" due to ambient temperature or pressure variations. Such breathing could introduce moisture inside the cable causing breakdown or impaired performance.

Air-articulated cables are best used in applications requiring low loss and/or low power-handling capability. Connector availability is limited. Teflon jacketing is available in lengths up to 25 feet.

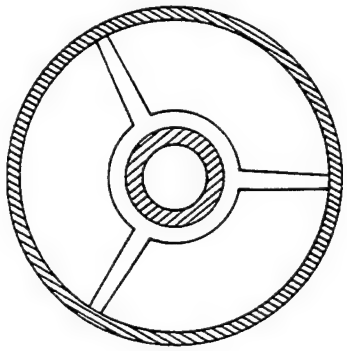

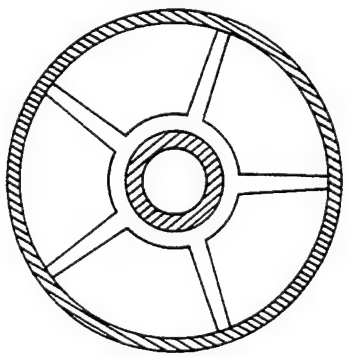

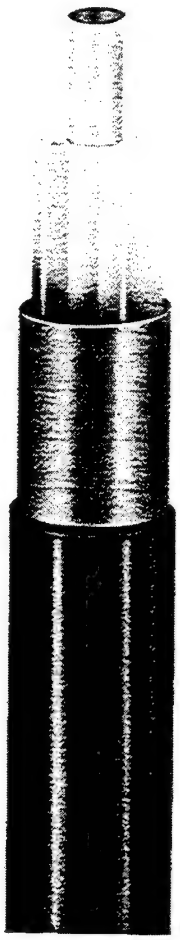

Figure 2

PRECISION TUBE COMPANY
North Wales, PA 19454 • 215/699-5801 • Telex 84-6439

Table II - Coaxial Cable Characteristics

Coax O.D. (in)	Coax O.D. (cm)	PTFE	ε_r (eff.) 300K/6K	Tan δ 300K/6K	O.D. Inner Conductor (cm)	I.D. Outer Conductor (cm)
0.085	0.216	Solid	2.1[(1)]/1.9[(2)]	2.0×10^{-4} [(1)]/2.4×10^{-6} [(2)]	0.051	0.168
0.085	0.216	Spline	1.3[(1)]	2.0×10^{-4} [(3)]/2.4×10^{-6} [(3)]	N/A	N/A
0.085	0.216	μPorous	1.3[(4)]	2×10^{-5} [(4)]/2.4×10^{-7} [(4)]	.070	0.168
0.141	0.358	Solid	2.1/1.9	2.0×10^{-4} /2.4×10^{-6}	0.091	0.298
0.141	0.358	Spline	1.3	2.0×10^{-4} /2.4×10^{-6}	0.114	0.298
0.141	0.358	μPorous	1.3	2×10^{-5}/2.4×10^{-7}	0.114[(5)]	0.298
0.250	0.635	Solid	2.1/1.9	2.0×10^{-4} /2.4×10^{-6}	0.163	0.530
0.250	0.635	Spline	1.3	2.0×10^{-4} /2.4×10^{-6}	0.221	0.530
0.250	0.635	μPorous	1.3	2×10^{-5}/2.4×10^{-7}	0.221	0.530
0.325	0.826	Solid	2.1/1.9	2.0×10^{-4} /2.4×10^{-6}	0.238	0.724
0.325	0.826	Spline	1.3	2.0×10^{-4} /2.4×10^{-6}	0.284	0.724
0.325	0.826	μPorous	1.3	2×10^{-5}/2.4×10^{-7}	0.284	0.724

Notes:

(1) From Precision Tube, Inc. and "Reference Data for Engineers", H. W. Sams & Co., 7th Ed.

(2) S. Isagawa, Jap. J. Appl. Phys. 15 (2059) 1976. Data taken is at 1.3K; we assumed not much change at 6 K.

(3) From Precision Tube, Inc. Measurements on their cables reveals no change in dielectric loss from solid PTFE.

(4) From Precision Tube, Inc. Tan δ values extracted from measured data. Scaled as per ref. (2) for 6 K.

(5) From Precision Tube, Inc. Micro-porous cable is being made with the same dimensions as air-articulated spline.

Table III - Niobium Coaxial Cable at 1 GHz

Maximum Operating Temp.: 6 K

$R_s = 1\ \mu\Omega$

Average Input Power = 50 W

Coax O.D. (in)	PTFE	Conductor Loss per cable (dB)	Dielectric Loss per cable (dB)	Total Loss per cable (dB)	Pwr. Loss per. 2000 lines (Watt)	Bundle (in. square)
0.085	Solid	1.5×10^{-3}	6.8×10^{-3}	8.3×10^{-3}	191	3.8
0.085	Spline	5.3×10^{-4}	5.6×10^{-3}	6.9×10^{-3}	160	3.8
0.085	μPorous	1.3×10^{-3}	5.6×10^{-4}	1.9×10^{-3}	46	3.8
0.141	Solid	8.7×10^{-4}	6.8×10^{-3}	7.6×10^{-3}	176	6.3
0.141	Spline	3.0×10^{-4}	5.6×10^{-3}	6.4×10^{-3}	146	6.3
0.141	μPorous	7.8×10^{-4}	5.6×10^{-4}	1.3×10^{-3}	30	6.3
0.250	Solid	4.9×10^{-4}	6.8×10^{-3}	7.3×10^{-3}	167	11.2
0.250	Spline	1.7×10^{-4}	5.6×10^{-3}	6.0×10^{-3}	139	11.2
0.250	μPorous	4.2×10^{-4}	5.6×10^{-4}	9.8×10^{-4}	23	11.2
0.325	Solid	3.6×10^{-4}	6.8×10^{-3}	7.1×10^{-3}	164	14.5
0.325	Spline	1.2×10^{-4}	5.6×10^{-3}	5.9×10^{-3}	136	14.5
0.325	μPorous	3.1×10^{-4}	5.6×10^{-4}	8.7×10^{-4}	20	14.5

Table IV - Cu Coaxial Cable at 300 K

Coax O.D. (in)	PTFE	Total Loss (dB/m)
0.085	Solid	0.62
0.085	Spline	0.51
0.085	μPorous	0.49
0.141	Solid	0.36
0.141	Spline	0.30
0.141	μPorous	0.28
0.250	Solid	0.21
0.250	Spline	0.18
0.250	μPorous	0.16
0.325	Solid	0.16
0.325	Spline	0.13
0.325	μPorous	0.12

From Table III, the micro-porous Teflon dielectric appears to offer the lowest loss and, therefore, the lowest heat dissipation. This would have to be confirmed experimentally in a follow-on effort.

Table IV shows calculations for room temperature Cu coaxial cable. For a maximum total cable length of approximately 30 ft. (10 m) (15 ft at the antenna end, plus 15 ft at the T/R module end), the 0.325 OD cable exceeds the 1 dB maximum loss specification by 0.2 dB. Larger OD cable would have to be used to provide acceptable loss, but this is not expected to present a problem.

Prediction Of High-Frequency Losses In Superconductors

Most of the loss in a superconductor can be placed in the following three categories: (a) loss due to the formation of vortices, (b) loss due to the existence of thermally produced "normal" electrons in the system, and (c) losses associated with the surface condition of the superconductor.

The loss listed under (a) is the origin of low-frequency hysteresis in a superconductor, which results macroscopically from bulk current and trapped flux, and microscopically from vortex movement and pinning centers. At high frequencies the movement can correspond not only to breaking loose from the pinning site, but also to cyclic bending of pinned flux lines and reversible motion. In principle, the loss (a) occurs when the RF magnetic field $H_{peak} > H_{c1}$, the superconducting lower critical magnetic field. Therefore superconducting cavities and transmission lines are usually designed with the restriction $H_{peak} < H_{c1}$. However, no catastrophe occurs when a few vortices are present and cavities with excellent quality factor Q have been made where H_{peak} exceeds H_{c1} [3,4]. Thus the vortex loss is generally not a critical factor if H is kept in the neighborhood of H_{c1}. At 500 W of peak power, the magnetic field on the surface of the inner conductor, where it is maximum, is approximately 12 Oe for a 0.141" OD cable. This is well below the critical field H_{c1} of Nb ($\cong$ 700 Oe at 6K)

At the zero of temperature, the loss due to (b) should vanish because the number of normal electrons vanishes for frequencies below the absorption edge observed at the energy gap frequency. But at finite temperatures and frequencies in the GHz range the normal electrons are generally the principal source of loss in a carefully prepared superconducting cavity. According to the widely accepted Bardeen-Cooper-Schrieffer (BCS) theory of superconductivity, the characteristic features of this loss at finite temperature are an f^2 dependence on frequency, and a temperature dependence given approximately by $e^{-\Delta/T}$ with Δ the superconductor energy gap. Thus within a given class of materials one can control this loss by operating at temperatures sufficiently below T_c, the superconducting critical temperature.

The loss (c) resulting from surface conditions depends upon both the chemical and mechanical conditions at the surface. This loss is generally assumed to lead to "residual" resistance, which does not follow f^2 behavior nor an exponential dependence on reciprocal temperature. In a cavity this loss has been successfully controlled by various polishing procedures [3,4,6,7], and by use of materials with stable surfaces.

Choice Of Superconductor

Among the ordinary superconductors, Nb has been the material of choice for low loss cavities and the same should apply for coaxial cables. Niobium has a relatively large T_c for ordinary superconductors, a small penetration depth λ, leading to a relatively high H_{c1}, and good surfaces of Nb can be prepared. However, for ease of construction, Pb has certain advantages, and considerable experience has been obtained using Pb-electroplated Cu and also Pb in thick sheets, which provide both a good surface and mechanical strength. Experimental coaxial cables are sometimes made using Nb for the inner conductor, and Pb for the outer conductor, but lowest loss surfaces are obtained with all-Nb cables. Recently, Nb sputtered on Cu has been tried in cavity systems, resulting in the low values of 42 nΩ of surface resistance [7].

Results for the surface resistance R_s for a superconductor come from cavity measurements, which vary considerably, but 1 $\mu\Omega$ at 4.2K and 1 GHz for Nb is easily obtained. Direct measurements of R_s for a superconducting coaxial cable are not available because of the loss in the dielectric, and because most such cables which have been constructed are short and have considerable losses in the leads. Losses much higher than expected have been found in a coaxial cable of Pb made in Japan [12], which gave 7×10^{-4} dB/m for the total attenuation at 1 GHz and 4.2K, but this high value seems to come from sources other than the superconductor. We have no reason to doubt that R_S values near 1 $\mu\Omega$ at 1 GHz can be obtained in coaxial cable made of Nb.

4. Cryogenic Considerations

The temperature of the coax lines must be maintained well below the superconducting critical temperature of Nb ($T_C = 9.1K$) in order to maintain a low R_S and correspondingly low power dissipation. The problem of cooling 2000 coaxial leads, each 75 ft in length, to temperatures below 6K is very similar to that faced in the design of large superconducting magnets. Immersing the lines in a bath of liquid helium at 4.2K, so-called "pool boiling", with the helium provided by a refrigerator, would be very difficult to accomplish owing to the geometry of the cable bundle. Also, it and would not provide uniform heat transfer along the length of the lines due to the presence of bubbles of gaseous helium. The most efficient and straight forward cooling scheme, which we

propose, is to enclose the lines in a sealed tube and use supercritical helium as the coolant. Helium in the supercritical state is a single phase fluid which will provide uniform heat transfer without the presence of bubbles formed by the vapor phase. This scheme has been used quite successfully for cooling high-current Nb_3Sn "rope-in-a-pipe" type conductors by Westinghouse in the construction of very large superconducting magnets. The supercritical helium would also be used to cool the transition regions at each end of the superconducting lines where they connect to the normal metal coax which then feed to the antenna at one end and the RF source at the other. Figure 1 shows a conceptual design of the system, which includes the antenna, coaxial lines from the cryogenic system to the antenna, a transition region in vacuum to reduce the heat load, and the superconducting lines at He temperatures. At the transmitter/receiver end there is a similar arrangement, with a conventional line going from the end of the cryogenic system to the T/R modules.

As an example, we consider 2000 coax lines, each 0.358 cm (0.141 in.) OD, packed in an approximately square array enclosed in a square stainless steel tube. The helium flow area through the interstices of the array is $(1-\pi/4)$ times the total cross-sectional area of the bundle, for this case about 55 cm^2. The required helium flow rate which will keep the outlet temperature of the coax sufficiently below T_C will, of course, be determined by the total power loss in the system. We chose 6 K as the allowable temperature of the warm end, since R_S (6 K, 1 GHz) $\cong$ 1 $\mu\Omega/\square$ for Nb, which is sufficiently small to allow the dielectric losses in the cable to dominate as shown in Section 3.

As a typical example to determine whether the operating conditions can be met, we assume that the coolant has an inlet temperature of 3.5K at a pressure of 3 atm. We find that a flow rate of 4.29×10^{-2} gm/sec/W will yield an exit temperature of 6K. From Table III, the calculated dissipation in 2000 lines made with the 0.141" OD cable with micro-porous Teflon dielectric is 30 W, for an input average power per line of 50 W. Assuming a more conservative 50 watts for the dissipation in the 2000 lines, a flow rate of 2.1 gm/sec would required. Under these conditions the flow is laminar with a Reynolds number << 2000 and a negligible pressure drop, $\Delta P < 10^{-3}$ atm. The friction losses associated with the flow are also negligible at $< 10^{-8}$ W. Even at 500 W of dissipation, corresponding to the 500 W peak input power per line, the required flow rate is 21 gm/sec, the flow remains laminar with $\Delta P < 10^{-3}$ atm, and the associated friction losses are $< 10^{-3}$ W.

Note that in the laminar flow range the friction factor is inversely proportional to the value of the Reynolds number which is a dimensionless quantity indicating the ratio of inertia forces to viscous forces, and is used to identify the flow regime. A low Reynolds number (Re < 2000) indicates laminar, or streamline, flow in which the fluid particles move along smooth paths or

laminae, with one layer sliding over an adjacent layer in a smooth, continuous path. A high Reynolds number ($Re > 10^4$) indicates turbulent flow where the particles move in a zigzag path transferring energy across streamlines. The correlations used to predict heat transfer and pressure drop in the two cases are substantially different.

The power dissipation in the coaxial lines occurs in both outer and inner conductors but predominantly in the dielectric. Good heat transfer from the outer conductor to the helium is assured by intimate contact and laminar flow conditions. However, we must also consider the transfer of internally generated heat to the coolant through the dielectric. At the peak power level of 500 W per line, the power dissipated in the center conductor and the dielectric is less than 250 mW (assuming a calculated 500 W of total loss in the 2000 lines). A standard thermal model for the temperature distribution in a cylinder with uniform internal heat generation may be used to calculate the temperature gradient across the dielectric. Assuming that the total power of 250 mW is uniformly distributed throughout the volume of the conductor, the corresponding power density along its length is $\cong 10^{-3}$ W/cm^3 . Using the published value for the thermal conductivity for Teflon $\kappa = 3 \times 10^{-4}$ W/cm/K at 4.2K, the thermal gradient between the inner and outer conductors is calculated to be < 0.05K, which is negligible.

Heat Leak At Lead Terminations

Calculations were also performed on the cooling capacity needed for 2000 conventional coaxial transitions from the superconducting lines to the room temperature region. As shown in Figure 1, a "coupling" region would exist between the conventional transition line in vacuum and the superconducting line. This can be a direct connection or a capacitive coupling, which would significantly reduce the heat load into the cryogenic system.

If we assume that a normally conducting lead made up of copper-clad stainless steel is used for the transition between room temperature and the superconducting lead, the heat leak through this lead into the supercritical helium must be determined. This heat leak was determined using a lumped parameter software model written in FORTRAN. The coaxial cable was assumed to be in a vacuum and was divided into 50 elements as shown in Figure 3. Elements 1 through 10 were assumed to be in the stainless steel inner conductor. Elements 11 though 20 were assumed to be in the copper layer on the stainless steel inner conductor. Elements 21 though 30 were assumed to be in the insulation between the inner and outer conductor. Elements 31 through 40 were assumed to be in a copper layer on the inner diameter of the outer conductor. Elements 41 through 50 were assumed to be in the stainless steel outer conductor.

Heat was assumed to be transferred between elements by conduction. Heat is generated in the two copper elements, and heat is transferred to the dewar wall from the outer stainless steel

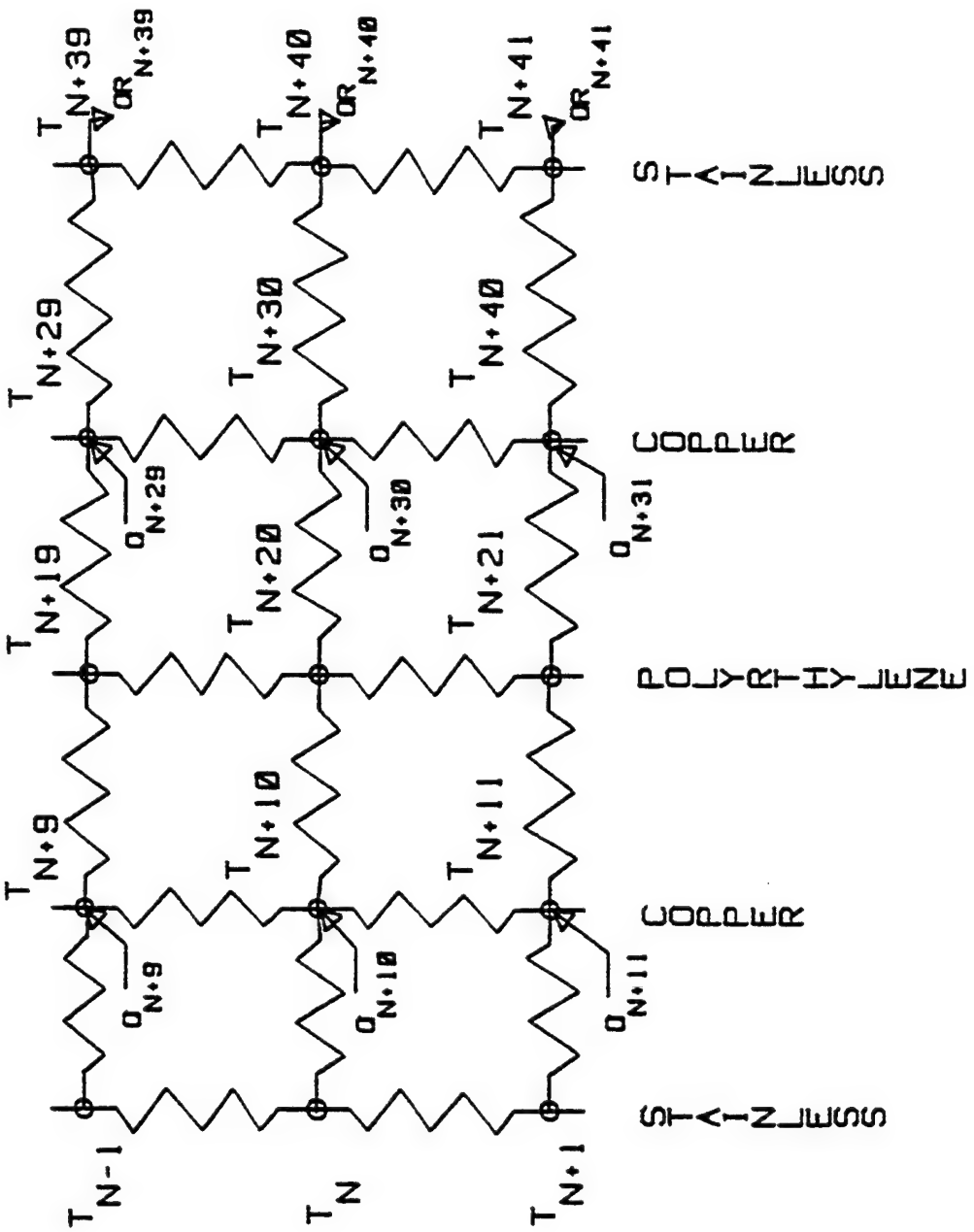

FIG 3. LUMPED PARAMETER MODEL

conductor by radiation. This results in 50 equations in 50 unknowns which can be solved to determine the temperature distribution and heat flows.

The copper was assumed to have a residual resistance ratio of 30. That means that the electrical resistivity of the copper at room temperature is 30 times the electrical resistivity of the copper at 4.2K. This is roughly equivalent to annealed OFHC copper. The thermal conductivity of copper as a function of temperature is shown in Figure 4.

The stainless steel was assumed to be ANSI 304. Its thermal conductivity as a function of temperature is shown in Figure 5.

The insulation was assumed to be polyethylene in this calculation. It was also assumed that other desirable dielectrics like PTFE (Teflon) do not have significantly different characteristics from polyethylene. The thermal conductivity of polyethylene as a function of temperature is shown in Figure 6.

The heat generated in the copper was assumed to be a linear function of temperature with a heat generation rate at 4.2K equal to one-half the heat generation rate at 300K. At higher temperatures the heat generation rate increases.

The radiation from the surface of the outer stainless steel conductor is given by:

$$Q_{rad} = \sigma \varepsilon A_1 \left(T_2^{\,4} - T_1^{\,4} \right) \qquad (1)$$

Where: Q_{rad} = Radiation heat flux, Watts

σ = Stefan-Boltzmann constant, Watt/cm^2-K^4

ε = Emissivity of surface, dimensionless

A_1 = Cold surface area, cm^2

T_2 = Temperature of dewar wall, K

T_1 = Temperature of conductor, K.

The emissivity of the surface, ε, is a function of temperature, as shown in Figure 7. The axial heat flow is given by:

$$Q_x = \frac{A_{xn}}{K_n L_n} (T_{n-1} - T_n) \qquad (2)$$

Where: Q_x = Axial heat flux, Watts

A_{xn} = Axial heat transfer area, cm

K_n = Thermal conductivity of element n, Watts/cm-K

FIG 4. THERMAL CONDUCTIVITY VS TEMPERATURE COPPER

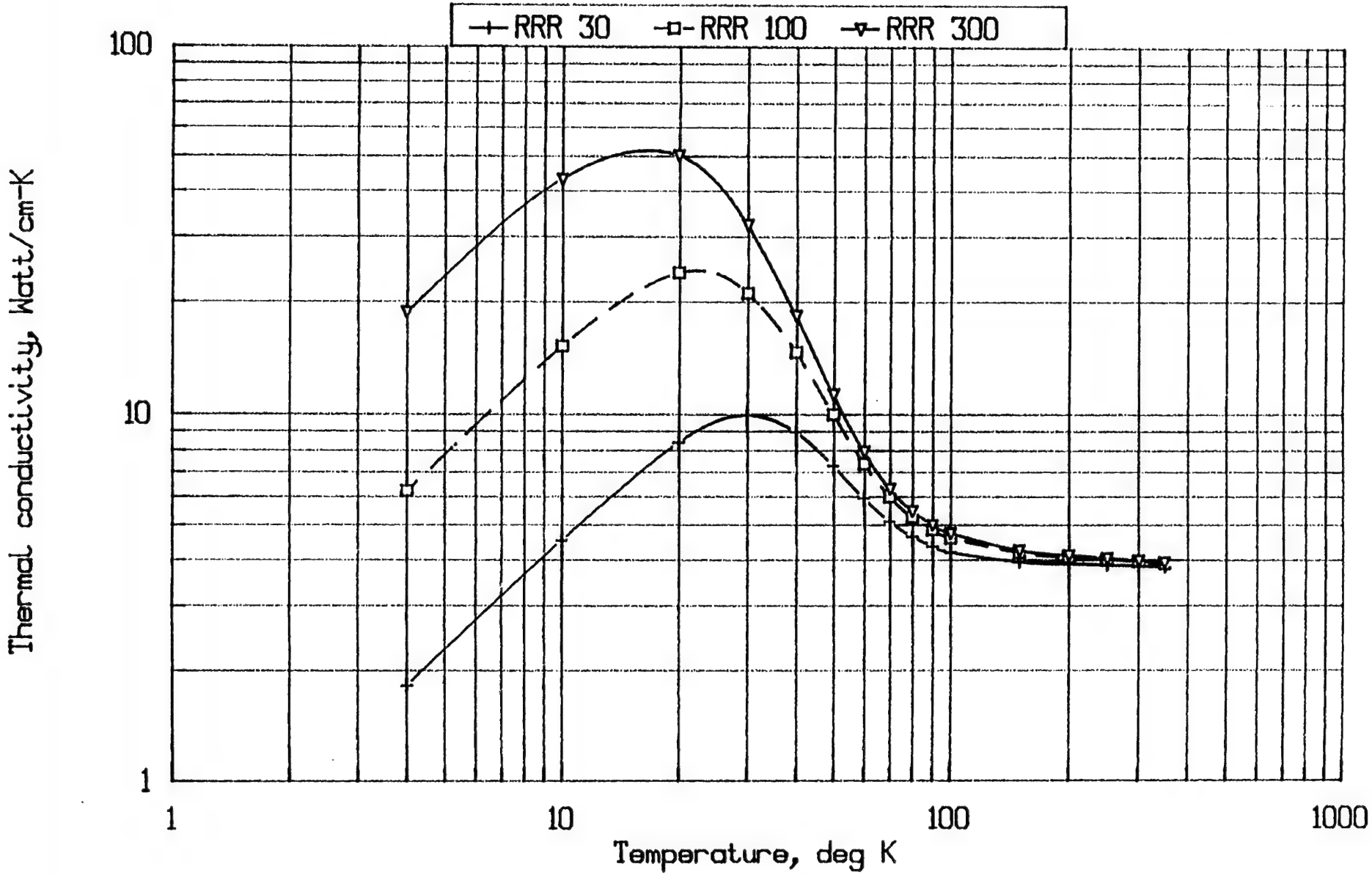

FIG 5.

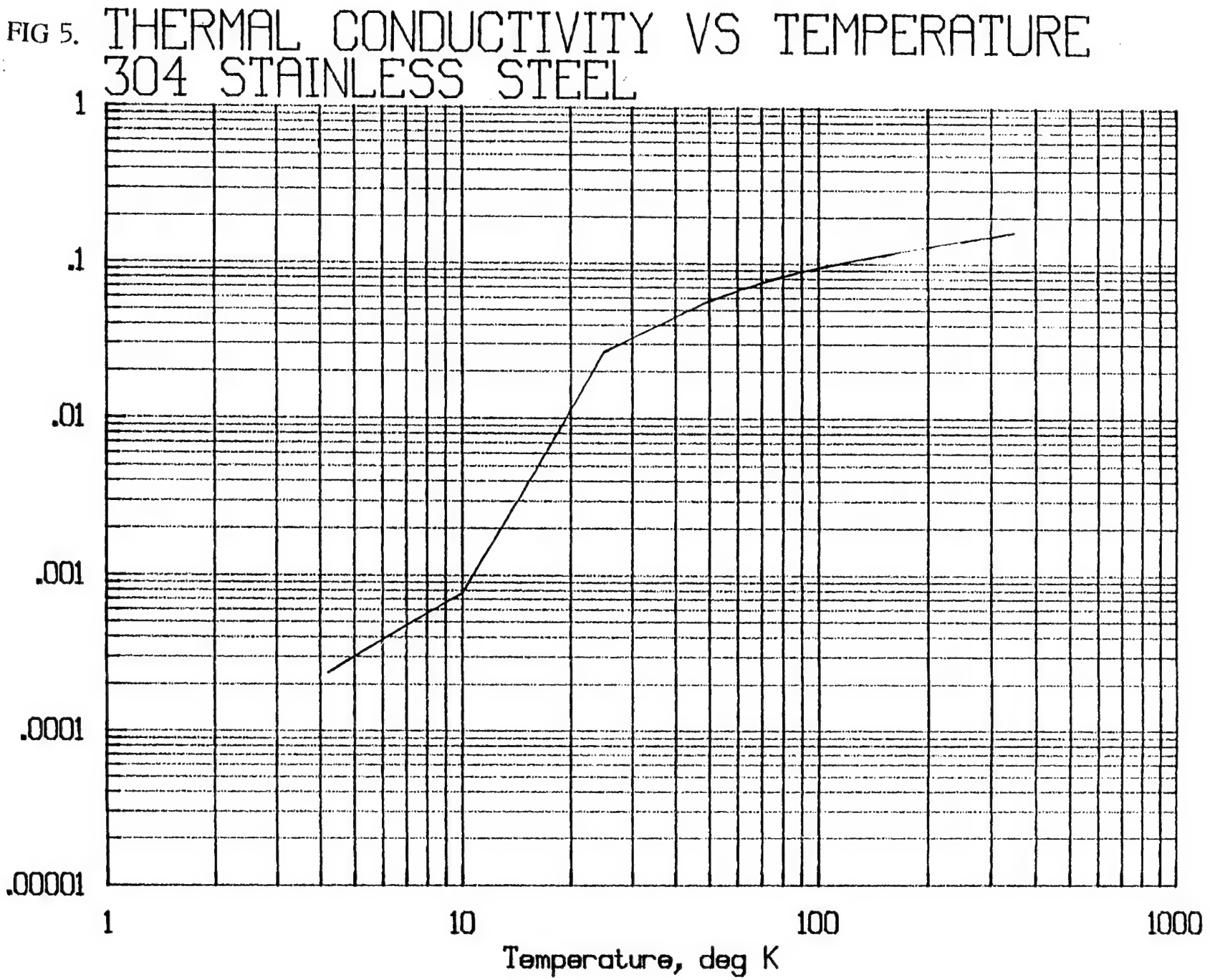
THERMAL CONDUCTIVITY VS TEMPERATURE
304 STAINLESS STEEL
1
.1
.01
.001
.0001
.00001
Thermal conductivity, Watt/cm-K
1
10
100
1000
Temperature, deg K

FIG 6.

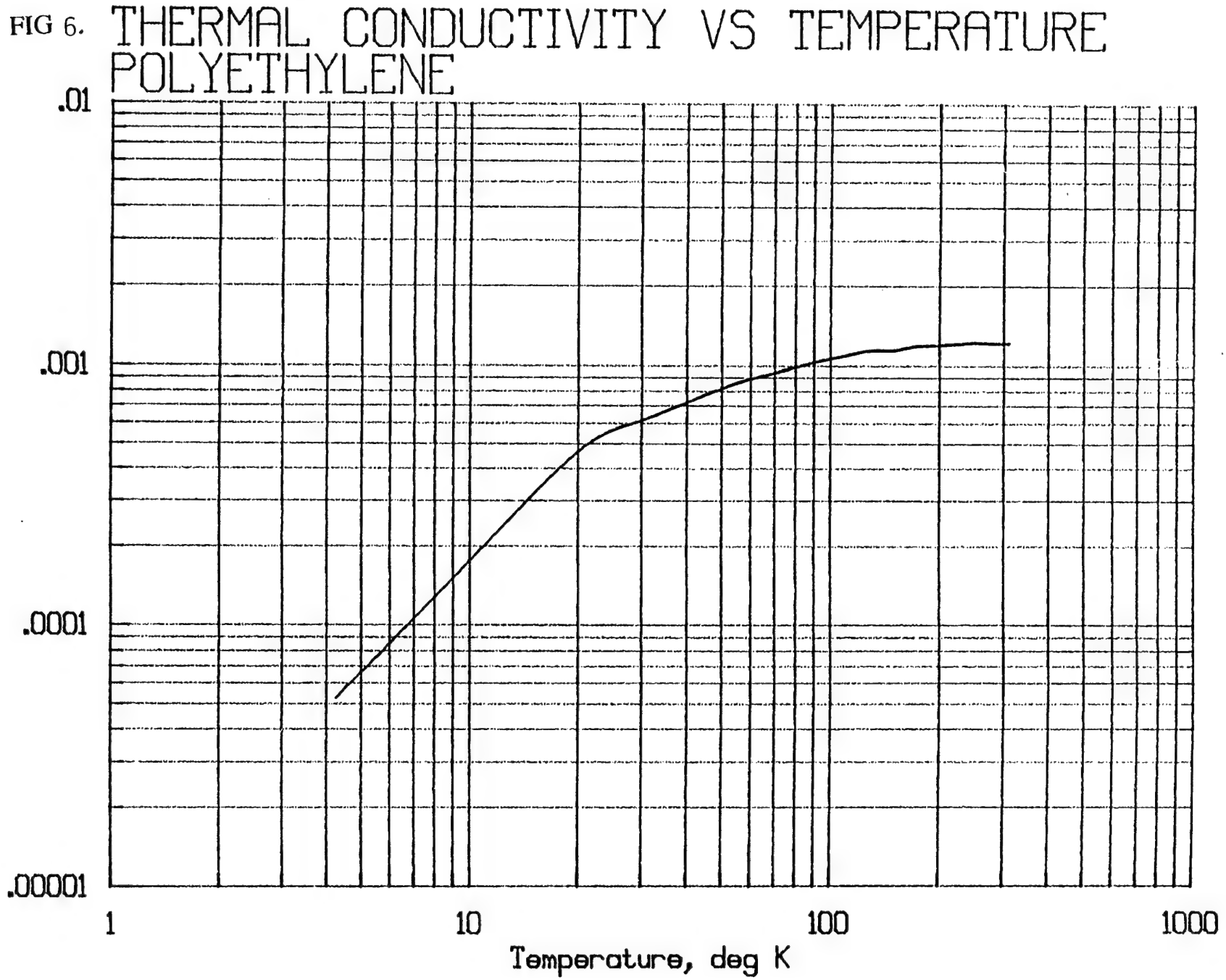
THERMAL CONDUCTIVITY VS TEMPERATURE
POLYETHYLENE
.01
.001
.0001
.00001
Thermal conductivity, Watt/cm-K
1
10
100
1000
Temperature, deg K

L_n = Length of element n, cm

T_{n-1} = Temperature of element n-1, K

T_n = Temperature of element n, K.

The radial heat flow is given by:

$$Q_r = \frac{2\pi K_n L_n}{\ln\left(\frac{r_n}{r_{n-10}}\right)}\left(T_n - T_{n-10}\right) \qquad (3)$$

Where: Q_r = Radial heat flux, Watts

K_n = Thermal conductivity of element n, Watts/cm-K

L_n = Length of element n, cm

r_n = Radius of element n, cm

r_{n-10} = Radius of element n-10, cm

T_n = Temperature of element n, K

T_{n-10} = Temperature of element n-10, K.

The lead geometry, lead warm-end and cold-end temperatures, and the heat generation rate at 300K were input to the program. A temperature distribution was assumed and the equations were solved. The calculated and assumed temperature distributions were compared. If the error in estimating any temperature exceeded 0.00001K (0.001%), the temperature estimate was adjusted and the temperatures were calculated again.

A coaxial cable with an outside diameter of 0.141 inches (0.358 cm) and a copper thickness equal to twice the skin depth at 300K were assumed and the program was run for various cable lengths. The calculated cold-end heat flux is shown in Figure 8 as a function of coaxial cable length. A typical distribution of temperature and heat generation rate is shown in Figure 9.

The cold-end heat flux per lead is a minimum of 0.17 Watts for a length of 2.6 inches (6.60 cm). For the two ends of 2000 lines, the total heat flux would be 680 Watts. This is well in excess of a realistic target refrigerator capacity of about 100 Watts.

Heat Leak With Capacitive Coupling

Capacitive coupling is routinely used in antenna design, especially in connection with rotary joints. Figure 10 shows a representative example of how capacitive coupling might be achieved in a coaxial configuration. This drawing is schematic, and does not represent an engineering

FIG 7. EMISSIVITY VS TEMPERATURE
304 STAINLESS STEEL

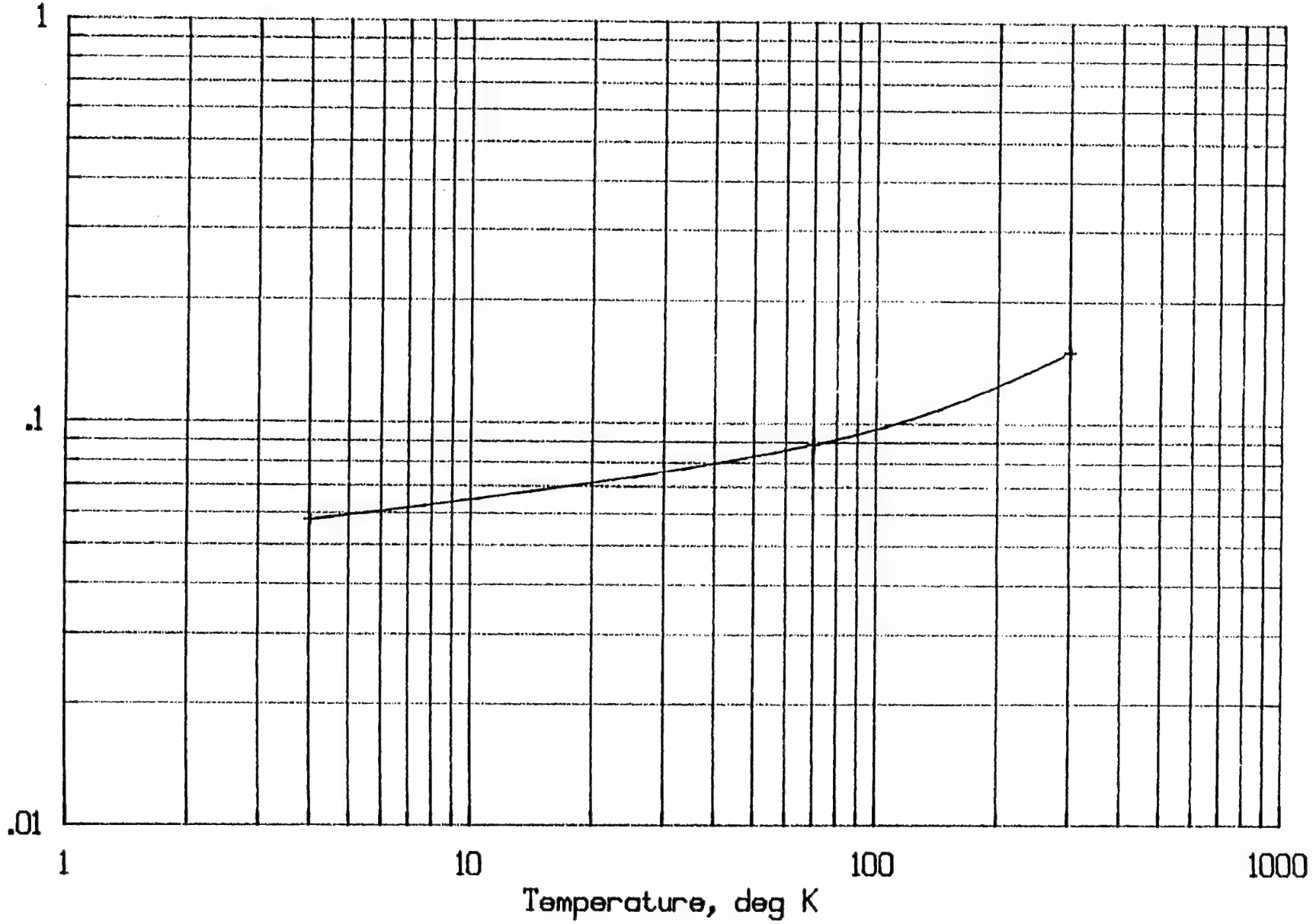

FIG 8.

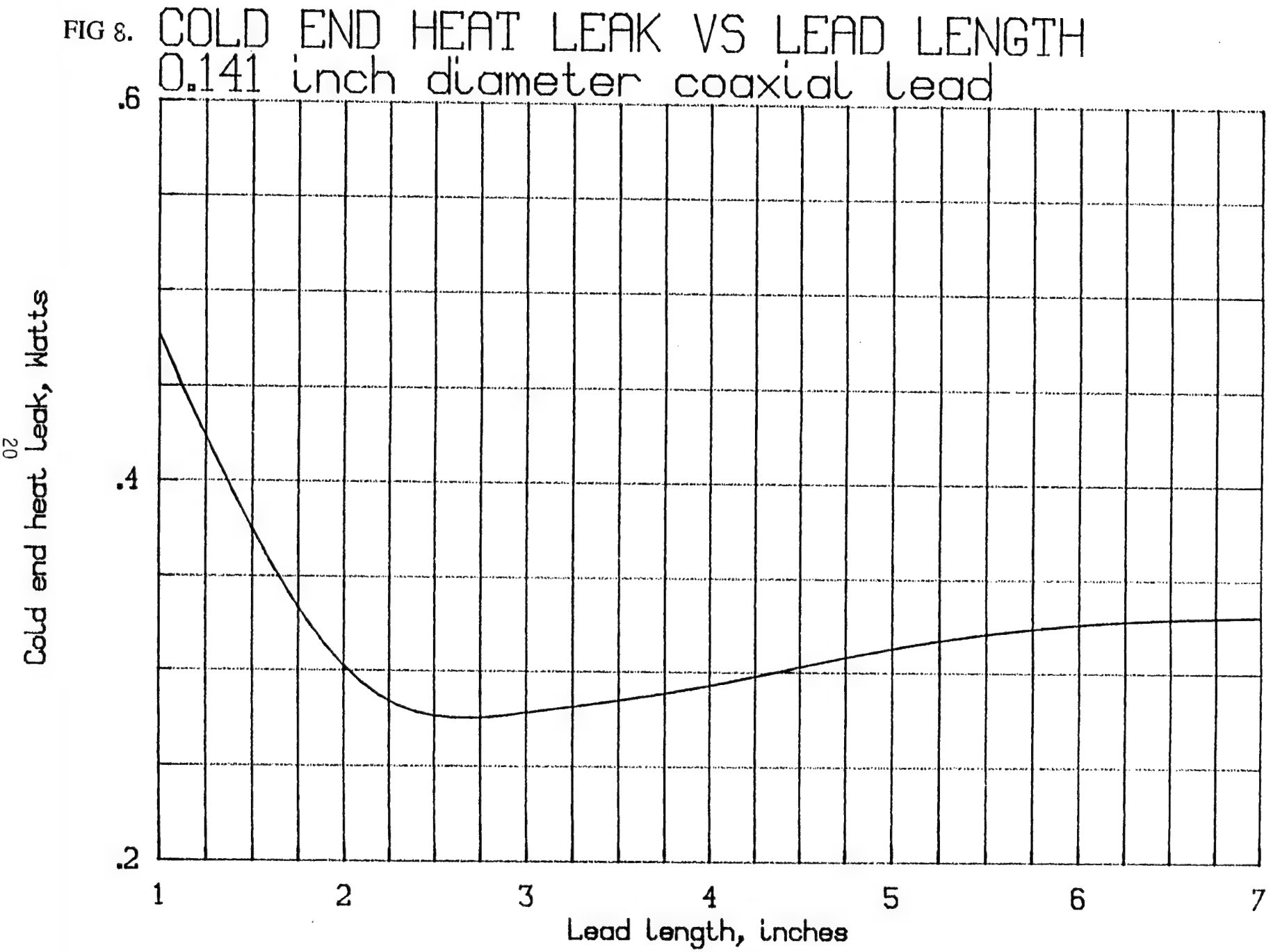
COLD END HEAT LEAK VS LEAD LENGTH
0.141 inch diameter coaxial lead
.6
.4
.2
Cold end heat Leak, Watts
1
2
3
4
5
6
7
Lead Length, inches

FIG 9. LEAD TEMPERATURE AND HEAT GENERATION RATE VS DISTANCE FROM WARM END

6 inch long lead

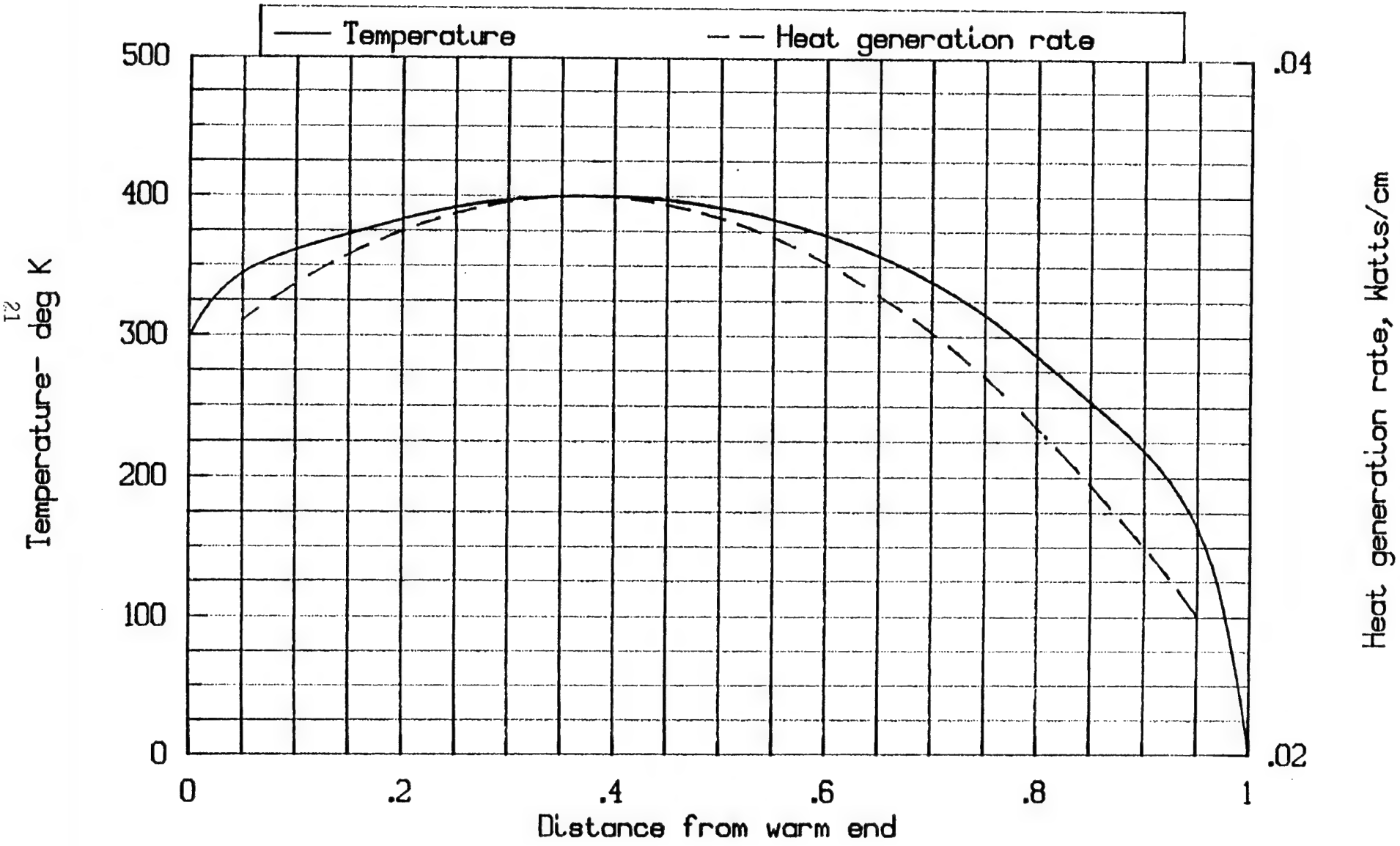

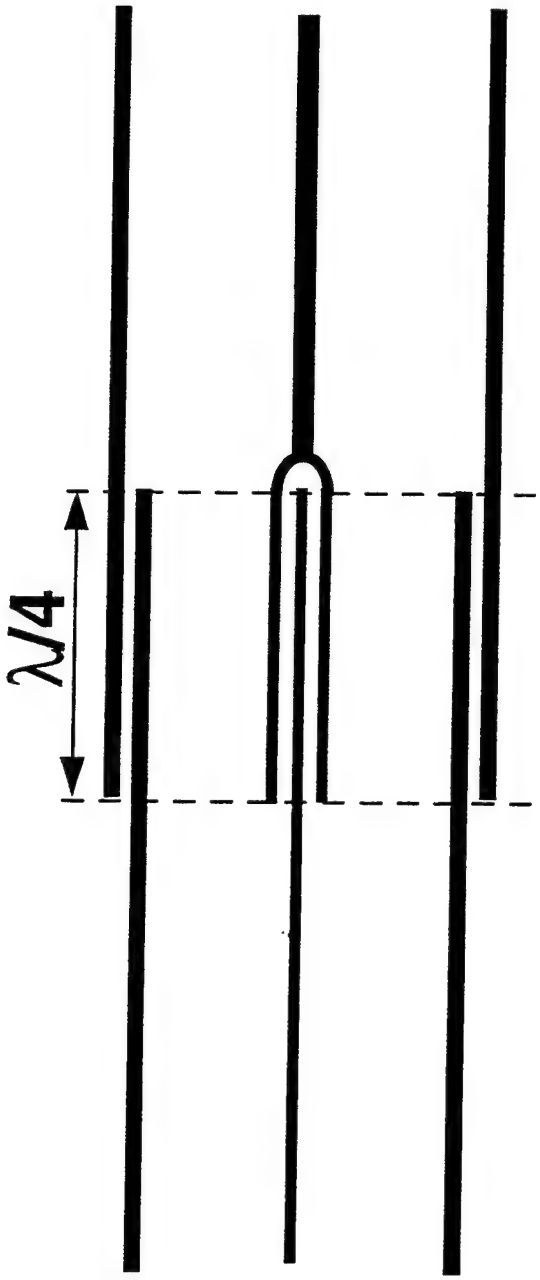

Figure 10

design. In the following thermal calculation, it was assumed that the structure can be engineered so that there is negligible heat load through a support structure that allows for the two sides of the coupling to be maintained in perfect alignment. In addition, as in the drawing in Figure 10, the dielectric in the capacitive coupling region is assumed to be vacuum, not a solid. It must be added that the engineering design of the system would have to be done so as to minimize any radiation leakage through the coupling region and the possible cross-talk between adjacent lines.

If we assume capacitive coupling, heat is transferred between the two parts of the coupling by thermal radiation and molecular gas conduction, as well as conduction through some form of supporting structure, which could be made of a good thermal insulator like the ceramic G-10. The heat transfer due to thermal radiation between two gray bodies is given by:

$$Q_{rad} = \sigma A_1 f_{12} (T_2^4 - T_1^4) \qquad (4)$$

Where: Q_{rad} = Thermal radiation heat flux, Watts

σ = Stefan-Boltzmann constant , 5.67 x 10^{-12} Watts/cm^2-K^4

A_1 = Area of cold surface, cm^2

f_{12} = Gray body shape factor, dimensionless

T_2 = Warm surface temperature, K

T_1 = Cold surface temperature, K.

The gray body shape factor is given by:

$$f_{12} = \frac{1}{(\frac{1}{\varepsilon_1} - 1) + \frac{A_1}{A_2}(\frac{1}{\varepsilon_2} - 1) + \frac{1}{F_{12}}} \qquad (5)$$

Where: ε_1 = Emissivity of cold surface, dimensionless

ε_2 = Emissivity of warm surface, dimensionless

A_2 = Area of warm surface, cm^2

F_{12} = View factor between surfaces

For a body completely enclosed by another body, F_{12} is unity. For polished aluminum at 300 K, Barron[13] gives ε as 0.03. At 4.2K Barron[13] gives ε as 0.015 for polished aluminum.

The heat transfer due to molecular gas conduction is given by:

$$Q_{gas} = \delta A_1 \frac{\alpha_1 \alpha_2}{\alpha_2 + \frac{A_1}{A_2}(1 - \alpha_2)\alpha_1} \frac{\gamma + 1}{\gamma - 1} \frac{P}{\sqrt{MT}} (T_2 - T_1) \qquad (6)$$

Where: Q_{gas} = Molecular gas conduction heat flux, Watts

δ = Constant, 2.426 x 10^{-3}

α_1 = Accommodation coefficient of cold surface, dimensionless

α_2 = Accommodation coefficient of warm surface, dimensionless

M = Molecular weight of gas

γ = Specific heat ratio of gas, dimensionless

P = Pressure of gas, Torr

T = Temperature of pressure measuring instrument, K.

The mean free path of the gas molecules must be greater than the spacing between the two surfaces for molecular conduction to occur. The mean free path is given by:

$$L = \phi \frac{\eta}{P} \sqrt{\frac{T}{M}} \qquad (7)$$

Where: L = Mean free path of gas molecules, cm

ϕ = Constant, 8.6 x 10^{3}

η = Viscosity of gas, poise.

Assuming helium is the residual gas, the molecular weight is 4.003 and the accommodation coefficient is 0.3 at 300K and 1.0 at 4.2K.

Assume the cold section of the capacitive coupler has an area of 1.0 cm^2, has a surface similar to polished aluminum and is at 6K. Assume the warm section of the capacitive coupler has an area of 2 cm^2, has a surface similar to polished aluminum and is at 300K or higher in temperature. The heat flux due to thermal radiation is shown in Table V.

Assume the residual gas is helium at a pressure of 1.0 x 10^{-5} Torr. The molecular conduction heat flux is also shown in Table V. The mean free path length is 1500 cm by Eq. 7, so molecular conduction will occur.

Since the surface area of the cold portion of the capacitive coupler will have an area of approximately 1 in^2 (6.5 cm^2) the heat flux will not exceed 0.001786 Watts/cm^2 x 6.5 cm^2 = 0.0116 Watts, giving a total heat flux of 0.0116 W x 4000 = 46.4 W, for the two ends of 2000 lines.

From Table III we find that the total loss in the cable bundle using 0.141" OD μPorous coaxial cable is estimated to be 30 W at an average RF input power level of 50 W per line. The total heat load, including the 46 W calculated for the transition regions using capacitive coupling, is therefore less than 100 W. A conservative 100 W of refrigeration capacity will be assumed to be required for this project, however. It must be pointed out again that a critical assumption was

made here for the coupling regions and that if a solid dielectric were used instead of vacuum (e.g. a good cryogenic thermal insulator like the ceramic G-10) the heat leak through the capacitive junction may be quite large.

Table V. Radiation and Molecular Conduction Heat Flux

Warm Temperature K	Thermal Radiation mW/cm^2	Molecular Conduction mW/cm^2	Total mW/cm^2
300	0.554	0.029	0.583
320	0.718	0.030	0.748
340	0.915	0.031	0.946
360	1.150	0.032	1.180
380	1.430	0.033	1.460
400	1.750	0.034	1.790

A candidate refrigerator was sought to determine whether the cooling requirements could be met with existing technology. Westinghouse STC has a refrigerator on site purchased from Process Systems International, Inc. (PSI) which is capable of providing supercritical helium at a flow rate of 4.9 gm/sec at 5.3K and 10 atm, or a cooling capacity of 64 W at 4.6K. This is a Model 1430 refrigerator with a single RS compressor. Figure 11 shows this system with the refrigerator in Figure 11(a) and the compressor in Figure 11(b). Figure 11(c) shows the manufacturer's specifications for the Model 1430 and Figure 11(d) the specifications for the RF compressor. At this inlet temperature and pressure, the flow rate required to yield an outlet temperature of 6 K is 0.327 gm/sec/W. The specified value of 4.9 gm/sec would provide just 15 W of cooling capacity, which clearly is not adequate. However, because this refrigerator represents current state-of-the-art, we queried PSI, Inc. to learn of other models and their specifications. As a result we have identified two possibilities.

By adding LN_2 precooling to the Model 1430 the cooling capacity is increased to 114 W at 4.6K. This system can then be used to extract the 100 W from the supercritical helium forced through the coaxial lines in a closed cycle by a separate pump. Under these conditions, the pump would be required to supply about 9 gm/sec at 4 atm to the RF system with an inlet temperature of 4.6 K and an outlet temperature of 6K.

A second option is the Model 1630 from PSI, Inc. with two RS compressors and LN_2 precooling. The Model 1630 specifications are shown in Figure 11(d). Informal, preliminary

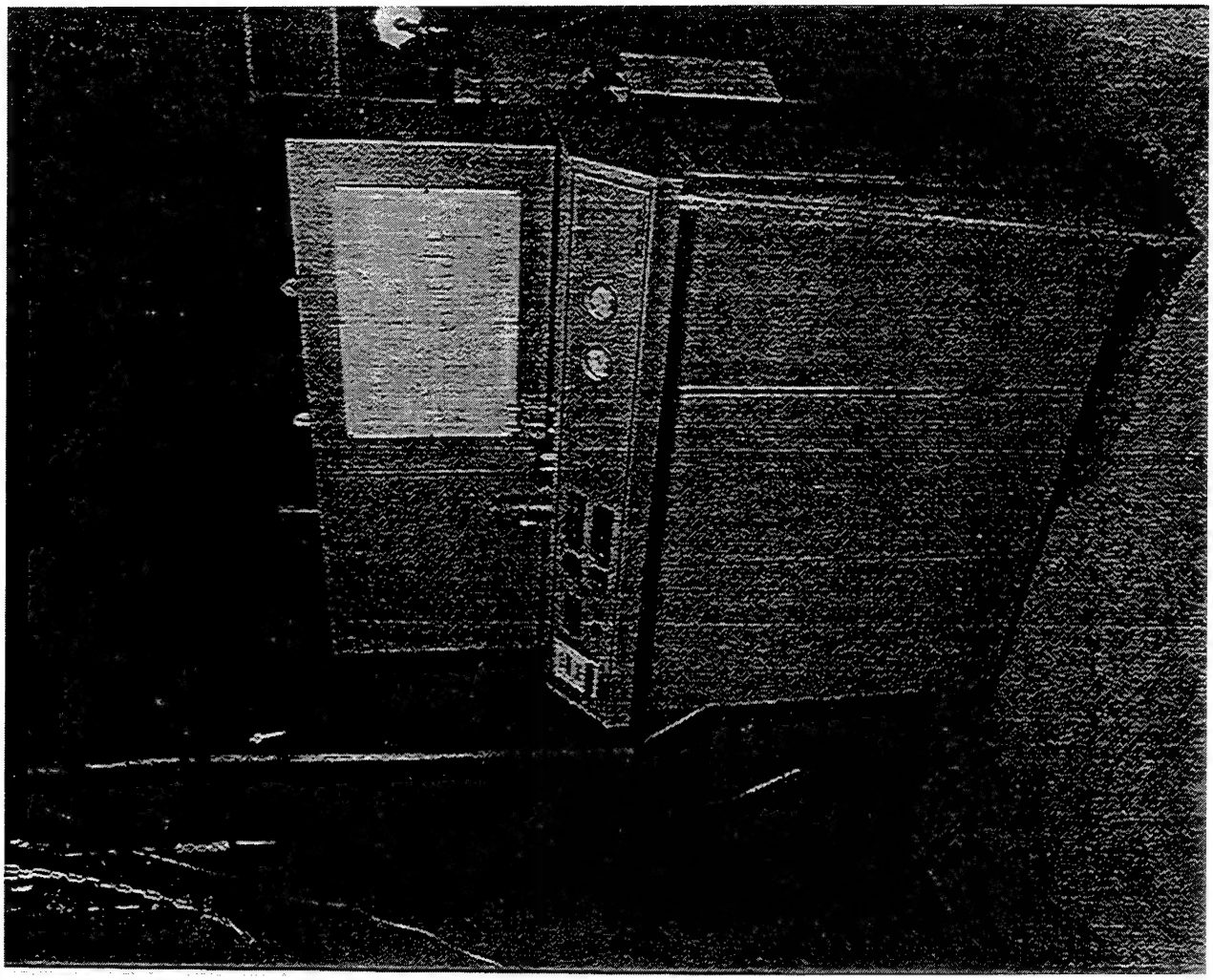

Figure 11(a)

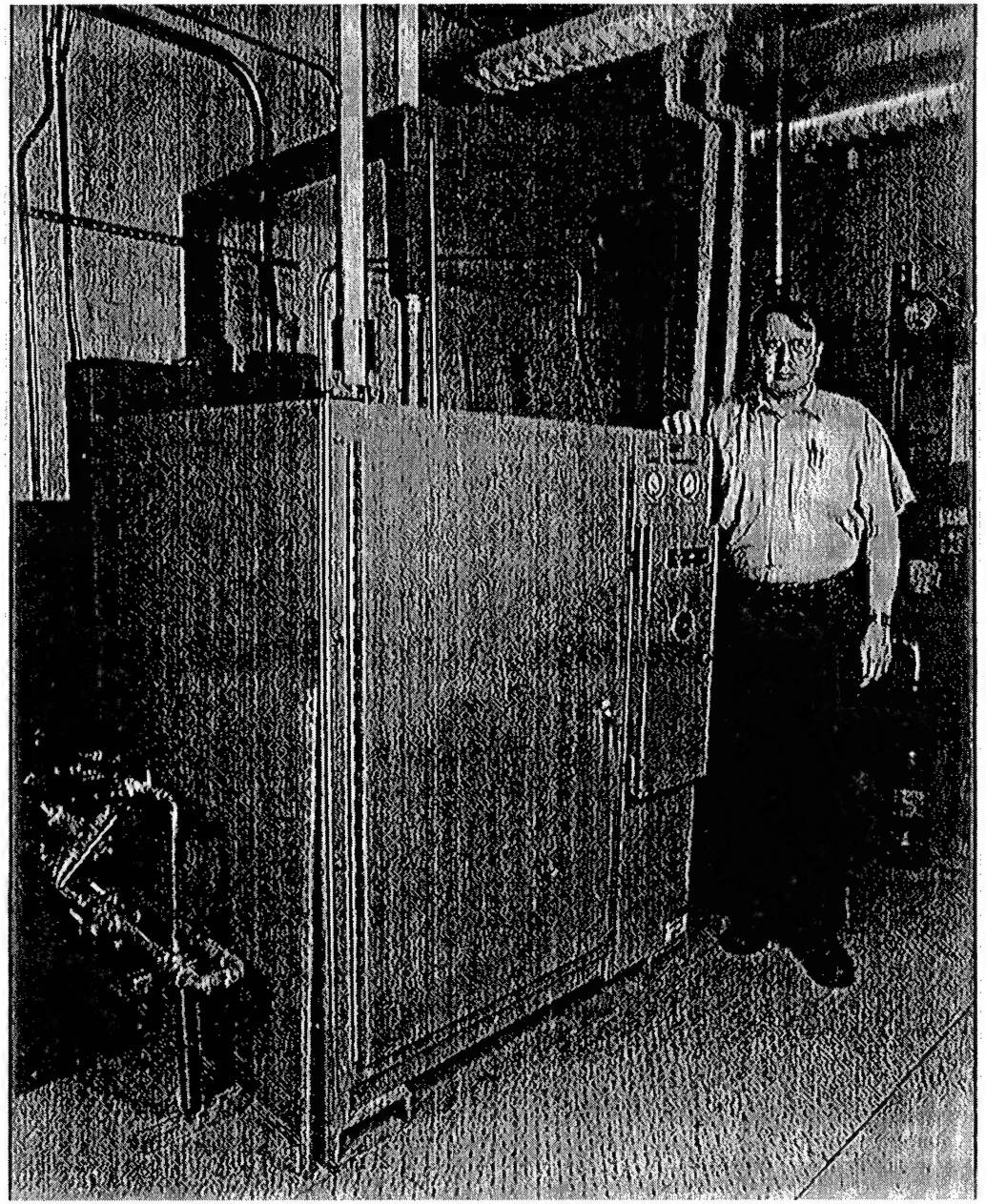

Figure 11(b)

SYSTEM SPECIFICATIONS

Basic SERIES 1400 helium Liquefaction/Refrigeration System consist of:

A. *One MODEL 1410, 1420 or 1430 Liquefier or Refrigerator Module*
Power: 20 amps, 220V, 1Ø, 50 or 60 Hz
Liquid Nitrogen (optional): 10 to 55 liters per hour
Overhead clearance required: approximately 10 feet (3050 mm)
Weight: 2200 lbs (1000 kg)

B. *One Model 1400 Compressor Module*
Power: 25 kW, 460V, 3Ø, 60 Hz, or 21 kW, 380V, 3Ø, 50 HZ
Cooling Water: 5 GPM (20 liters/minute) at 75°F (24°C) and 3 atm pressure
Weight: 1800 lbs (816 kg)

C. *One Remote Delivery Tube (MODELS 1410, 1430)*
56 inches (1422 mm) Horizontal Length

D. *Two sets of Operation/Maintenance Manuals and Installations/Interface Drawings*

Alternates

One MODEL RS Helium Compressor, Module
Power: 100 kW, 460V, 3Ø, 60 Hz, or 83kW, 380V, 3Ø, 50 Hz
Cooling Water: 20 GPM, (80 liters/minute) at 75°F (24°C) and 3 atm pressure
Weight: 3200 lbs (1455 kg)

MODEL 1410 LIQUEFIER
MODEL 1420 REFRIGERATOR
MODEL 1430 REFRIGERATOR

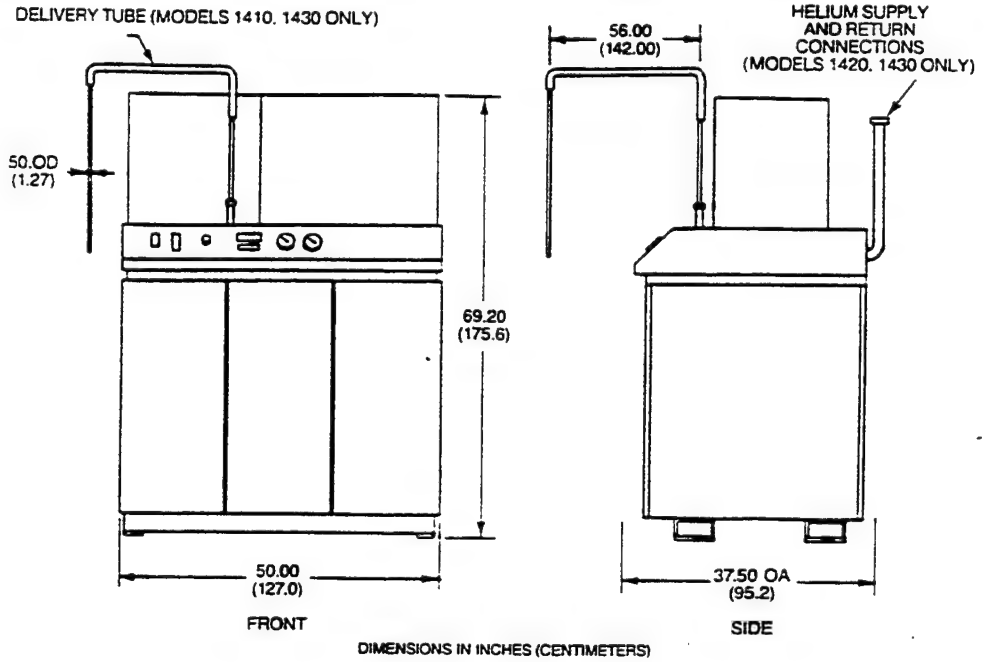

DIMENSIONS IN INCHES (CENTIMETERS)

MODEL 1400 COMPRESSOR

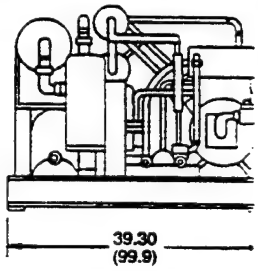

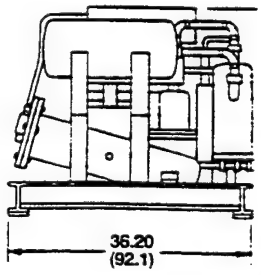

Process Systems International, Inc.
20 Walkup Drive
Westborough, MA 01581-5003
(508) 366-9111 FAX (508) 870-5930

DCN-0

Figure 11(c)

01581-5003 USA • TLX 200294 • FAX 508-870-5930 • Telephone 508-366-

SYSTEM SPECIFICATIONS

SERIES 1600 Helium Liquefaction/Refrigeration System consisting of:

A. *One MODEL 1610, 1620 or 1630 Liquefier or Refrigerator Module*
Power: 20 amps, 120V, 1 ϕ, 50 or 60 Hz
Liquid Nitrogen (optional): 10 to 70 liters per hour
Overhead clearance required: approximately 10 feet (3050 mm)
Weight: 2100 lbs. (955 kg)

B. *One MODEL RS Helium Compressor Module*
Power: 100 kW, 460V, 3 ϕ, 60 Hz, or 83 kW, 380V, 3 ϕ, 50 Hz
Cooling Water: 12 GPM (46 liters/minute) at 75°F (24°C) and 3 atm pressure
Weight: 2000 lbs. (910 kg)

C. *One Remote Delivery Tube (MODELS 1610, 1630)*
56 inches (1422 mm) Horizontal Length

D. *Two sets of Operation/Maintenance Manuals and Installation/Interface Drawings*

Alternate:
One MODEL 1400 Compressor Module
Power: 25 kW, 460V, 3 ϕ, 60 Hz, or 21 kW, 380V, 3 ϕ, 50 Hz
Cooling Water: 5 GPM (20 liters/minute) at 75°F (24°C) and 3 atm pressure
Weight: 1800 lbs. (816 kg)

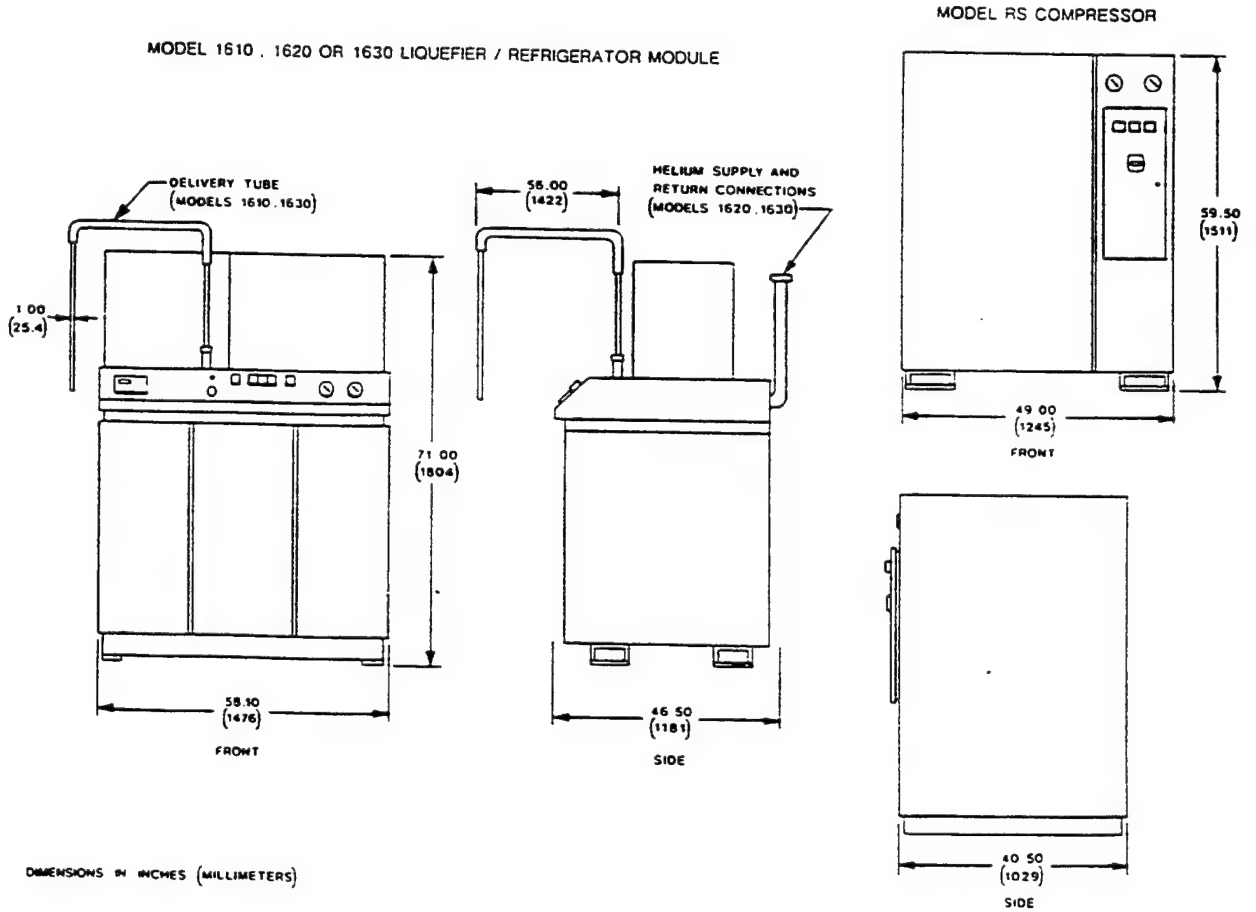

PROCESS SYSTEMS INTERNATIONAL, INC.
20 Walkup Drive
Westborough, MA 01581-5003
(508) 366-9111 FAX (508) 870-5930

Figure 11(d)

estimates from PSI, Inc. are that this system would provide approximately 15 gm/sec at 5.1K and 4 atm, or a cooling capacity of 210 W. Although this system is significantly larger in volume and weight than the 1430/pump option, it would provide more margin, having about twice the required capacity.

There are, of course, many other refrigerator suppliers which should be consulted if there is further interest. However, for the purpose of this study we believe that the estimates of physical size and cooling capacity provided by the PSI, Inc. models are representative of the state-of-the-art.

5. Study Issues Addressed

The following is a concluding list of the issues this effort was intended to address, as per our contractual obligations with NRL. Some of these issues have already been discussed in the preceding sections, but are summarized here for completeness.

Superconducting Materials

This study was carried out using niobium as a representative material. It is a well understood metallic superconductor whose electrical, mechanical and thermal properties are well known. Tubes and wires of the proper dimensions for coaxial cable manufacture can be obtained [14] in sufficiently high quality (i.e. surface resistance ≤ 1 $\mu\Omega$ at 6K and 1 GHz, H_{c1} of several hundred Oersted at 6K) to provide the superconducting properties required. Furthermore, the attractive possibility exists of using Nb-clad stainless steel coaxial cable (see next item, below), which would provide the electrical characteristics needed in combination with the mechanical strength and low heat conductivity of stainless steel. Another option which could be explored in a follow-on effort is Pb-coated Cu, as explained in Section 3.

Transmission Line Configuration

The preferred transmission line configuration for this application is coaxial cable. It provides wide band characteristics, isolation between lines, small cross-section, mature manufacturing technology, is scaleable to other frequency bands, and it offers the low loss required. As explained above, its basic components, superconducting tube and wire, can be obtained commercially, at least for the case of niobium. An attractive alternative to solid Nb tube and wire, is Nb cladding of stainless steel tube and wire. We have contacted Accumetrics [15], a manufacturer of tubing for coaxial cable fabrication and a supplier to Precision Tube, Inc. [16], a leading maker of semirigid coaxial cable. Accumetrics claims prior work using Nb and other refractory metals and proposes to use a Nb/Cu cladding on stainless steel tube and wire and to fabricate the coaxial cable jointly with Precision Tube, Inc. This would be cheaper than solid Nb

tube and wire, and would benefit from the mechanical strength of stainless steel and its low thermal conductivity, as well as from an established manufacturing process.

Lead-plated copper is also an alternate possibility for this application.

RF Power Handling Capabilities

Our calculations on thermal and electrical characteristics of the superconducting transmission line show that the 500 W of peak power can be handled, from both the cooling point of view and the superconducting properties, i.e. the RF field will remain much smaller than H_{C1}.

Transition from Superconducting to Normal Transmission Lines

The calculated heat loss through standard coaxial connections is far too high for practical refrigerators. Capacitive coupling is recommended in order to avoid conductive heat losses. This is acceptable for antenna applications and is used routinely in rotary junctions, for example. However, implementation in a cryogenic coaxial line system will require a careful design to avoid excessive heat leak through the support structure for the alignment of the capacitively-coupled joints. A preliminary calculation shows excessive heat loss through a solid dielectric if it were used between the cold and warm ends of the capacitive joint. Therefore, the joints have to be designed for vacuum dielectric with a support and alignment structure that minimizes the heat loss. In addition to the required careful electrical design to minimize reflections over the bandwidth of interest, the radiation losses through the capacitive coupling joint and the possible attendant cross-coupling between adjacent lines must also be minimized. **In conclusion, the transitions from superconducting to normal lines are a critical area that will require thorough examination in any feasibility demonstration of this concept.**

Cooling Requirements, Type and Cost

The use of forced-flow supercritical helium to maintain the cryogenic temperature of the superconducting coaxial lines is the method of choice. A great deal of experience has been gained by industry in designing and constructing large superconducting magnets using this cooling technique. The estimated 100 W of maximum cooling power required may be provided by a state-of-the-art helium refrigerator. Two examples from Process Systems International, Inc [17] have been cited. (1) The Model 1430 without LN_2 precooling is shown in Figures 11(a) and (b). Manufacturer's specifications are given in Figures 11(c) and 11(d). This unit with LN_2 precooling and an auxiliary pump added would accomplish the task by providing 114 W at 4.6K, or a margin of 14%. The approximate cost for the Model 1430 is $310K. (Installation, auxiliary pump, and precooling not included). (2) The Model 1630 shown in Figure 11(d) is about 10 inches larger in linear dimension than the Model 1430. With two RS compressors, [one is shown in Figure 11(b)], and LN_2 precooling, this model would provide approximately 210 W at 4.6K, or a margin of 100%.

The approximate cost for the Model 1630 is $450K. These two examples are intended to show the minimum required and that which would provide twice the necessary refrigeration power. This study has been by no means complete. If there is further interest, other vendors should be consulted for competitive examples. Cost estimates are based on informal quotes from Process Systems International, Inc.

Manufacturing

Manufacturing of niobium coaxial lines can be performed in a similar fashion to coaxial cable with conventional materials. Informally, Precision Tube Company, Inc. has informed us that if niobium tube and wire of the proper dimensions were supplied, it is very likely that the cables can be made using existing equipment and techniques. Nb tubes and wires of dimensions approximating those required for the coaxial cable under consideration can be fabricated. However, the dimensional tolerances which may be achieved with Nb compared to other materials must be determined, since variations in conductor diameter along its length will play a role in determining the electrical properties of the coax. Another important requirement of the manufacturing process will be the consistent production of Nb tube and wire with good surface quality. This will be an important factor even though in the calculations presented here the dielectric losses dominate over the losses in the Nb surfaces.

As explained above, however, the technique proposed by Accumetrics of using Nb/Cu-clad stainless steel could be the most practical and economic way to manufacture the system. It will be explored further if there is interest.

Experimental Demonstration

One of the important parameters used in this study, but not firmly documented, is the dielectric loss in the coaxial cable at cryogenic temperatures. This should be determined early on in any feasibility demonstration. We propose that a subsize system incorporating approximately ten superconducting cables should be fabricated and tested. The subsize system must be of sufficient length to predict the performance of the full size system. We propose that length to be about 3 m. A prototype of the transition regions, including capacitive coupling, tested with the subsize bundle will predict the performance required for the final system.

Cost

Based on the assumptions made in this study the cost of the refrigerator required for this system ranges between $350K and $500K. This price range was obtained from informal estimates by PSI, Inc. [17]. The estimated cost of an experimental feasibility demonstration with a subsize cable bundle has been studied by Accumetrics with inputs from Precision Tube and from Teledyne-Wah Chang, a supplier of Nb material. However, their estimate was not available at the

time of this writing and will be supplied to NRL as a separate document once it is received. The feasibility demonstration would not require the purchase of a PSI refrigerator because a Model 1430 unit (Figure 11) is available to us at the Westinghouse Science and Technology Center.

Not enough information exists as yet for a realistic estimation of the cost of the entire system and therefore it will not be attempted at this time.

6. References

1. S. Isagawa, Jap. J. Appl. Phys. 15 (2059) 1976.
2. C. Rose and M. J. Gans, IEEE Trans. on Microwave Theory Tech. 38 (166) 1990.
3. H. Pfister, Cryogenics, Jan. 1976, p. 17.
4. M. Tigner, IEEE Trans. Mag. 15, 15, 1979.
5. C. Durand et al., IEEE Trans. on Appl. Superconductivity 5, 1107, 1995.
6. H. Lengeler, Cryogenics, Aug. 1998, p. 465.
7. V. Palmieri et al., IEEE Trans. On Appl. Superconductivity 3, 193, 1993.
8. P. Fabbricatore et al., IEEE Trans. On Appl. Superconductivity 3, 197, 1993.
9. N. Krause et al., IEEE Trans. MAG-17, 927, 1981.
10. P. Kneisel, O. Stoltz, and J. Halbritter, IEEE Trans. MAG-15, 21, 1979.
11. A. J. Cummings and A. R. Wilson, "New Techniques for Superconducting Cables," paper provided by Talisa.
12. N. Chiba, Y. Kashiwayanagi, and K. Mikoshiba, Proc. IEEE, Jan. 1973, p. 124.
13. R. Barron, "Cryogenic Systems," McGraw-Hill Inc., New York, 1966.
14. Goodfellow, Inc., Berwyn, PA 19312; Teledyne-Wah Chang, Oregon.
15. Accumetrics, Inc.; Paul Pitcher, contact. Tel. 610-948-0181.
16. Precision Tube Company, Inc; Anson West, contact. Tel. 410-546-3911.
17. Process Systems International, Inc.; Michael Pickett, contact. Tel. 508-898-0369.

Figure Captions

Figure 1 - Schematic drawing of the superconducting transmission line system and its connections to the antenna and the transmit-receive modules.

Figure 2 - Sample cross-sectional drawings of the air articulated coaxial cable using Teflon as the dielectric. Taken from the Precision Tube, Inc. coaxial cable catalog.

Figure 3 - Lumped parameter model.

Figure 4 - Thermal conductivity vs temperature copper.

Figure 5 - Thermal conductivity vs temperature 304 stainless steel.

Figure 6 - Thermal conductivity vs temperature polyethylene.

Figure 7 - Emissivity vs temperature 304 stainless steel.

Figure 8 - Cold end heat leak vs lead length 0.141 inch diameter coaxial lead.

Figure 9 - Lead temperature and heat generation rate vs distance from warm end 6-inch long lead.

Figure 10 - Schematic drawing of a representative example of a capacitive coupling section in a coaxial configuration. Transitions of this type will be required to reduce the heat loss between the warm and cold ends of the transmission line system.

Figure 11 - (a) Process Systems International, Inc. Model 1430 He refrigerator at the Westinghouse Science and Technology Center in Pittsburgh. (b) RS compressor. (c) Manufacturer's specifications for Model 1430. (D) Manufacturers specifications for Model 1630 and RS compressor.